

# Innovative characterization of magmatic domains: parametric inversion of finite- element models at Eyjafjallajökull volcano, and adapted level-set shape optimization

*Tutor*

Karine Lavernhe

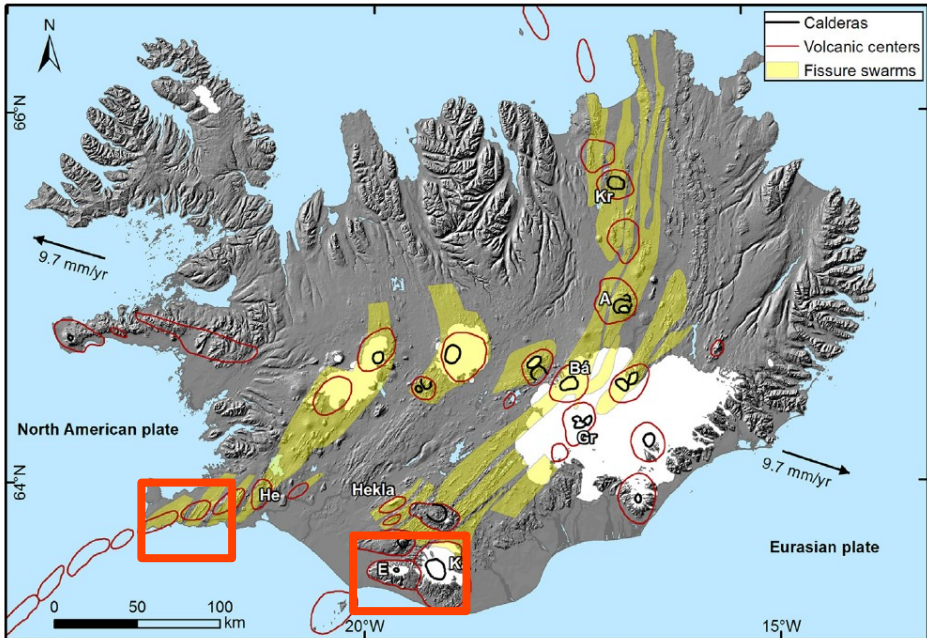
Théo Perrot

*Main supervisor*

Freysteinn Sigmundsson

# Introduction - Volcanology of Iceland

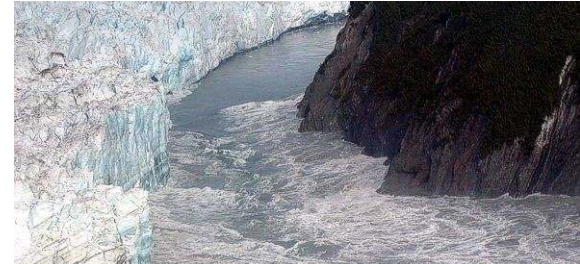
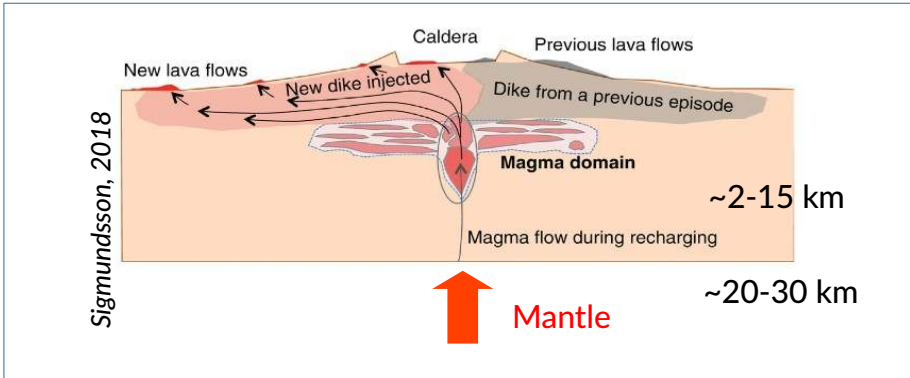
Sigmundsson, 2007



- Mid-atlantic ridge + hotspot = Iceland
- 32 active volcanic systems
- Subglacials volcanoes

- Magma formed at the mantle
- Uprises with buoyancy
- Stored in magma domain
- $P > P_c \Rightarrow$  eruption

→ Where and how are the magmatic reservoirs feeding a given volcanic system ?



- Eruptions
  - Earthquakes
  - Lava flows
  - Gaz plumes
  - Glacier floods



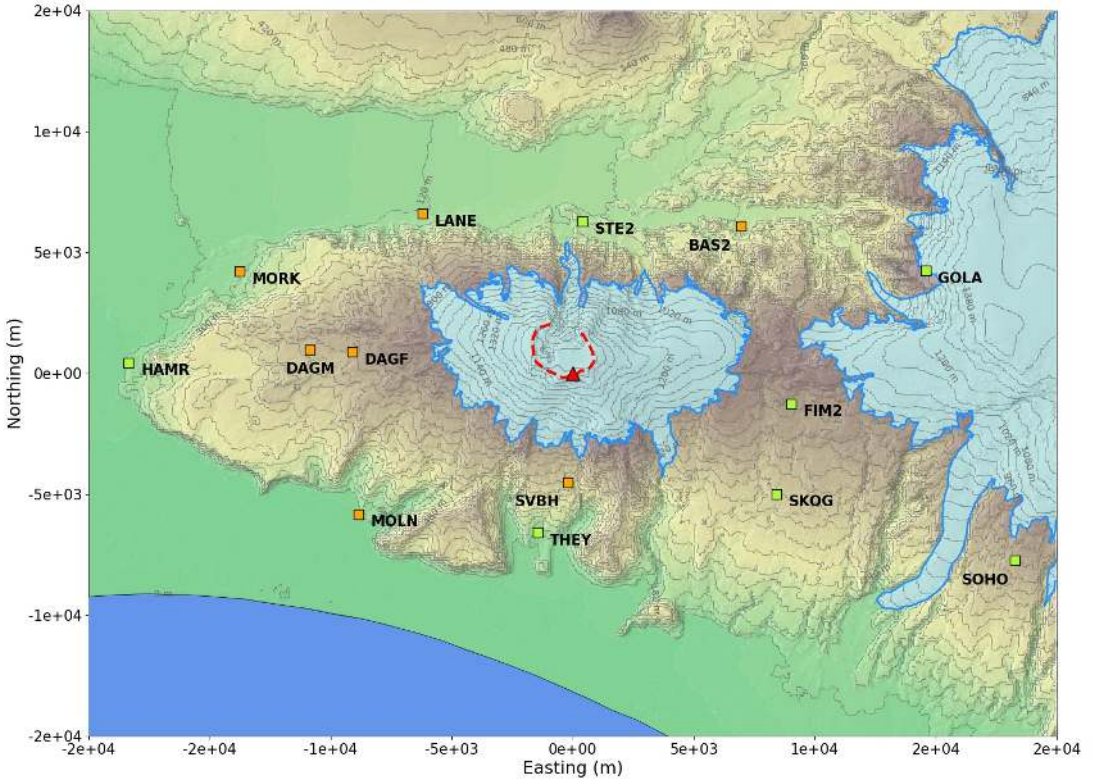
# I

## Parametric optimization of finite-element models of an inflation at **Eyjafjallajökull**

*North view of  
Eyjafjallajökull volcano  
taken from Þórsmörk*

# Context

- Central volcano
  - Inside EU plate => cold
  - No fissure swarm
  - E-W elongated (20km)
  - 1670 m high
  - Subglacial
  - Summit caldera
- Eruptive activity
  - 4 historical eruptions
  - Each preceding Katla eruption
- 2010 eruption
  - 20 years of unrest
  - March : Small effusive eruption on flank
  - April : Explosive eruption at the summit



How was the ground deformation at Eyjafjallajökull volcano in the 2011-2023 period and what processes caused these movements ?

# Monitoring tools

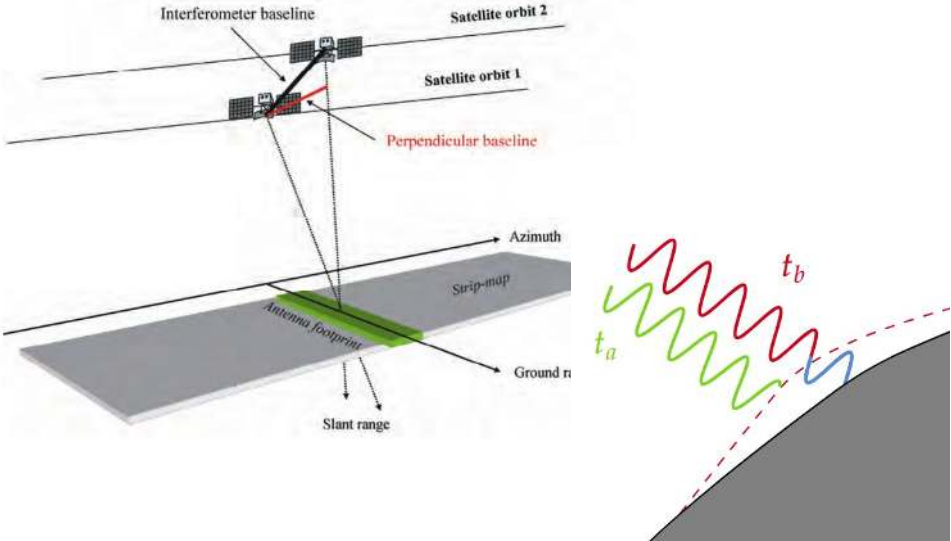
## Global Navigation Satellite System (GNSS)



- ⊕ temporal resolution ~8h-1day
- ⊕ 3D components
- ⊕ precision ~5mm
- ⊖ area coverage
- ⊖ atmospheric perturbation
- ⊖ maintenance

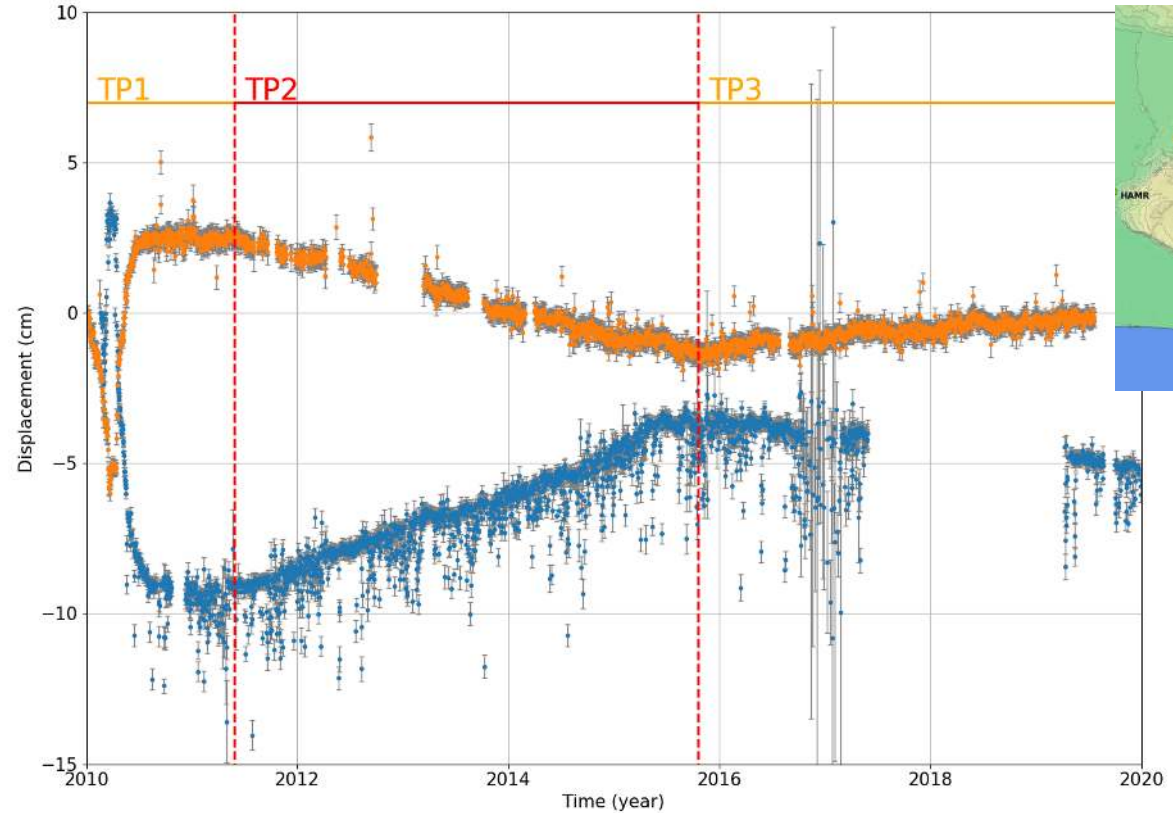
## Interferometric Synthetic Aperture Radar (InSAR)

Fletcher, 2007



- ⊕ area coverage
- ⊕ precision ~5mm
- ⊖ 1D
- ⊖ temporal resolution
- ⊖ atmospheric perturbation

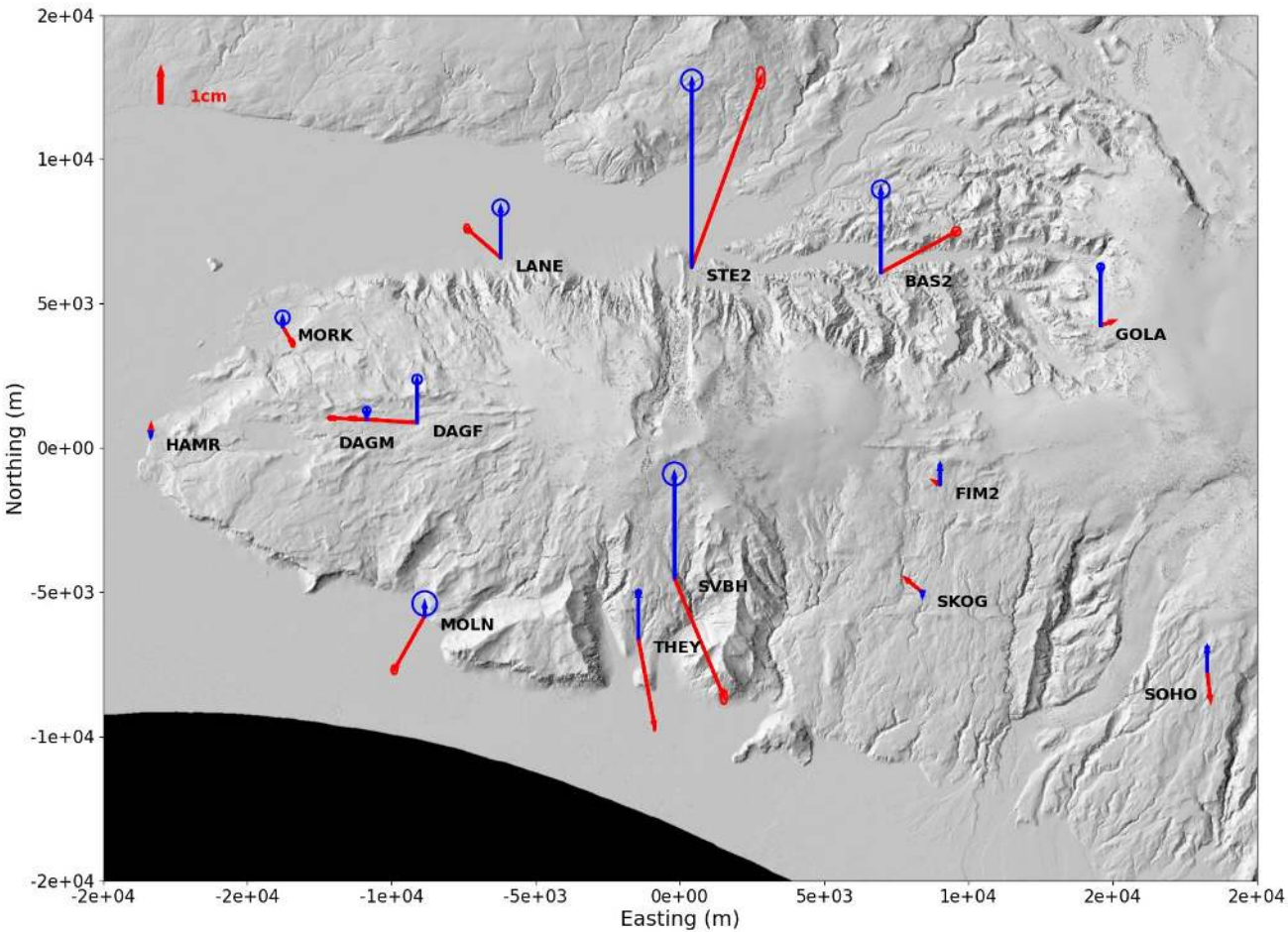
# Observations - GNSS



- TP1 : inflation and deflation, april 2010 eruption
- TP2 : Linear inflation ~2011-2015
- TP3 : Linear deflation 2015-now

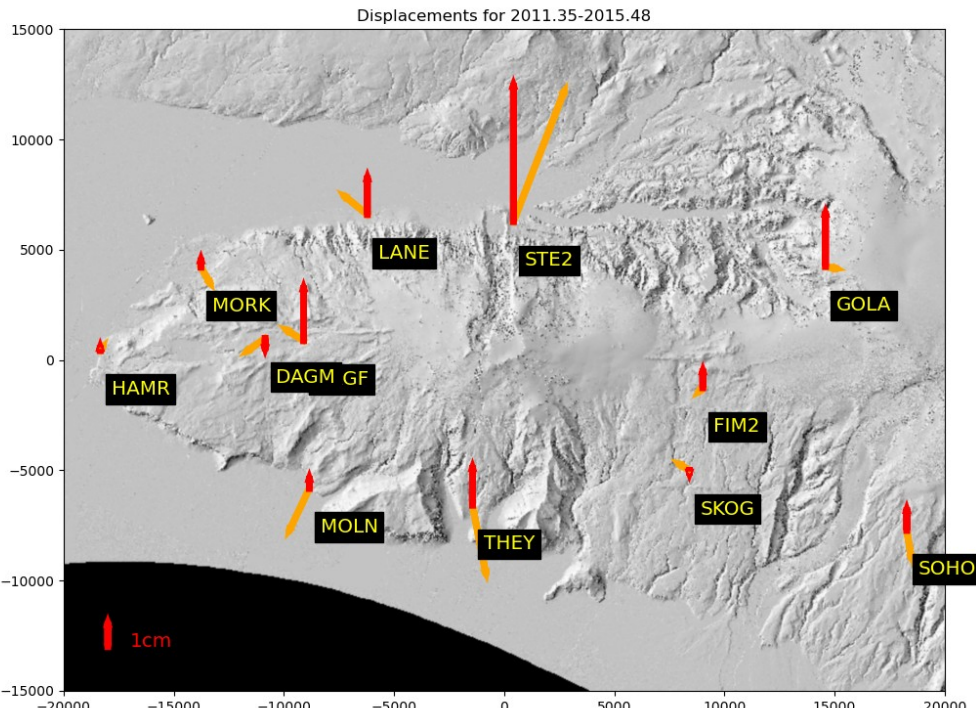
=> total displacement is studied =>linear elasticity

# Observations - GNSS

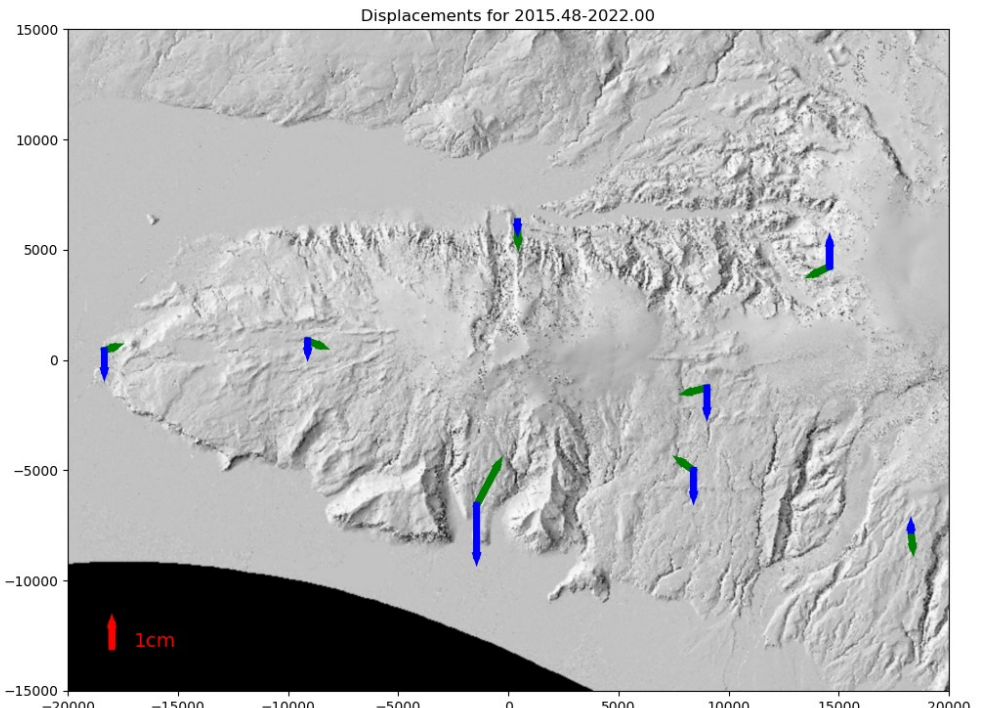


- 2011-2015 total inflation
- Pre-processing
- Detrended % Eurasian plate (E,N)
- Local Katla phenomenon removed (E,N)
- Glacial Isostatic Adjustment removed (U)

# Observations - GNSS



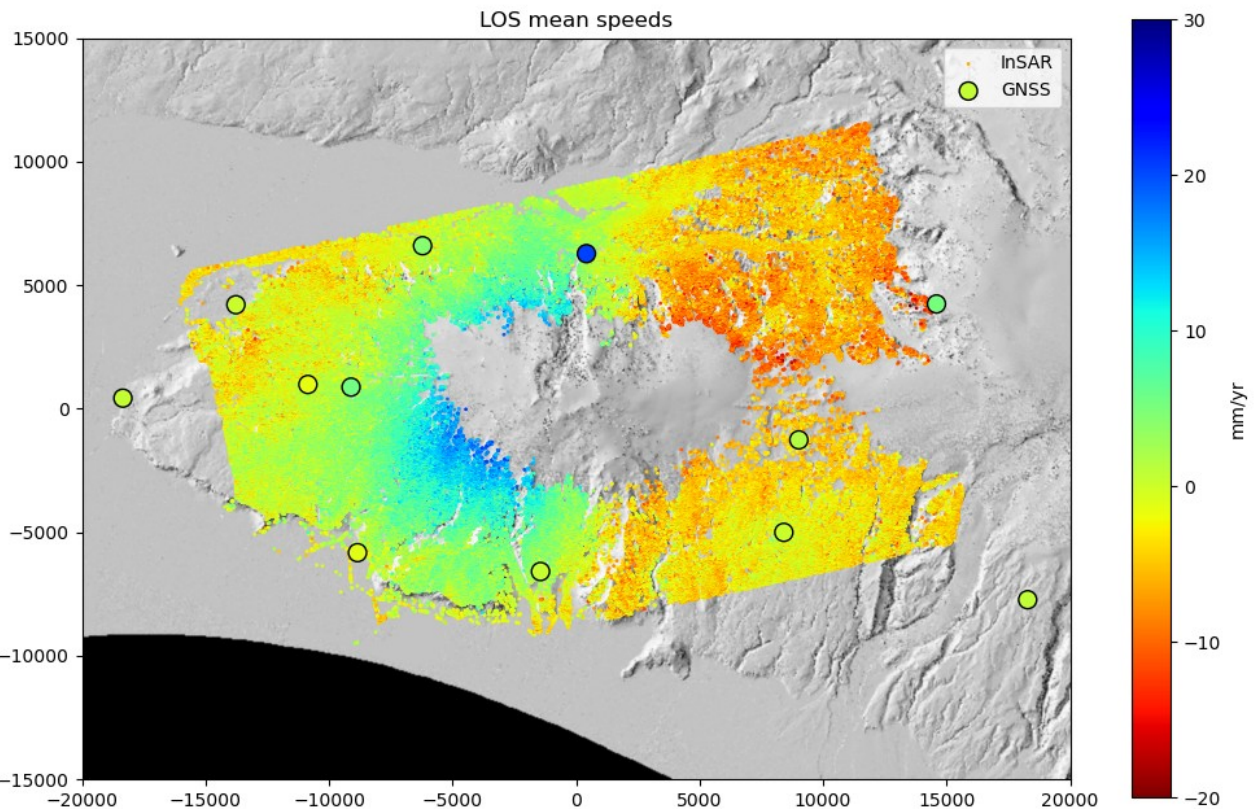
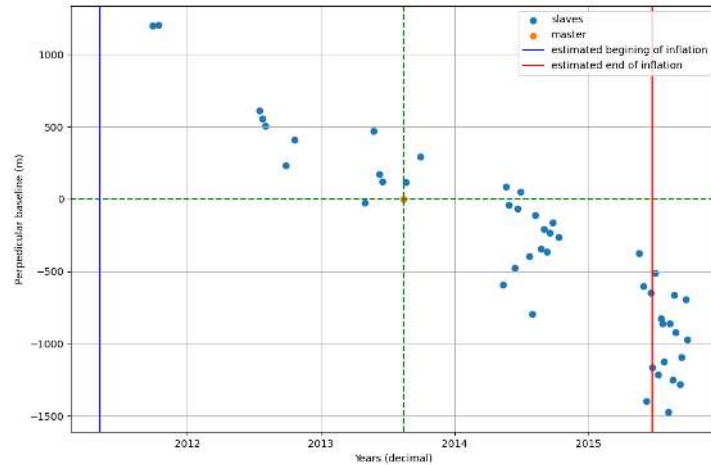
Inflation clearly visible  
=> main focus of this work



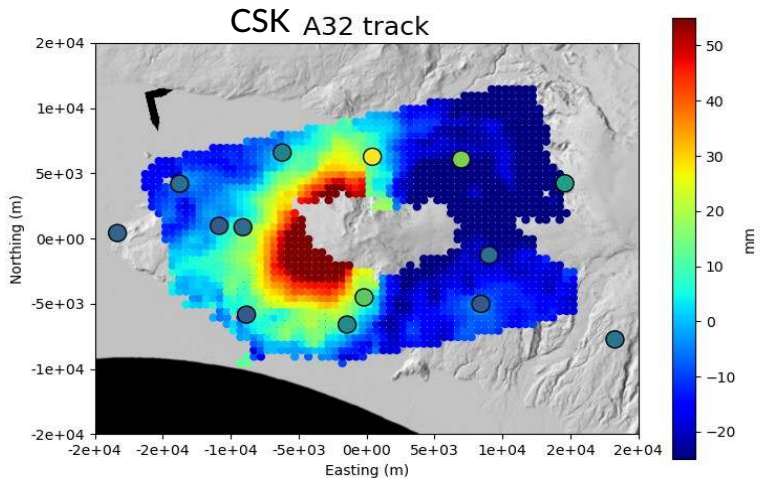
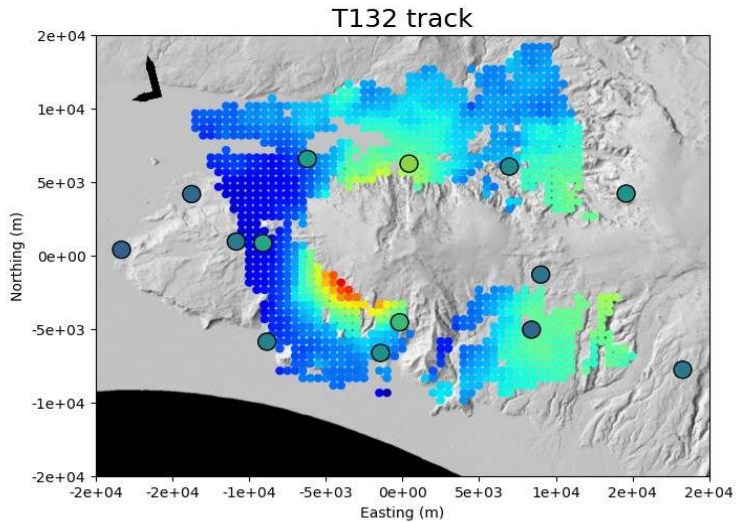
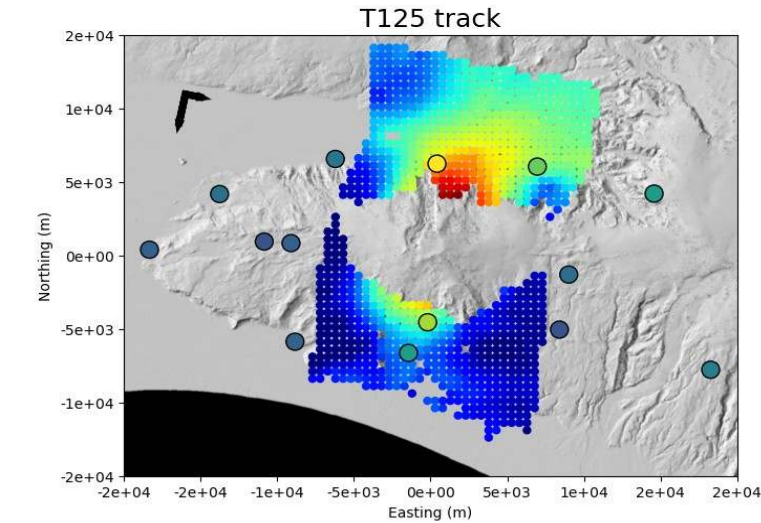
Small deflation signal  
=> need further investigation

# Observations - InSAR

- Cosmo SkyMed Ascending track 32
- Time-serie processing using StAMPS
  - Filtering interferograms
- => average speed 2011-2015
- Corelates well GNSS data



# Observations - InSAR



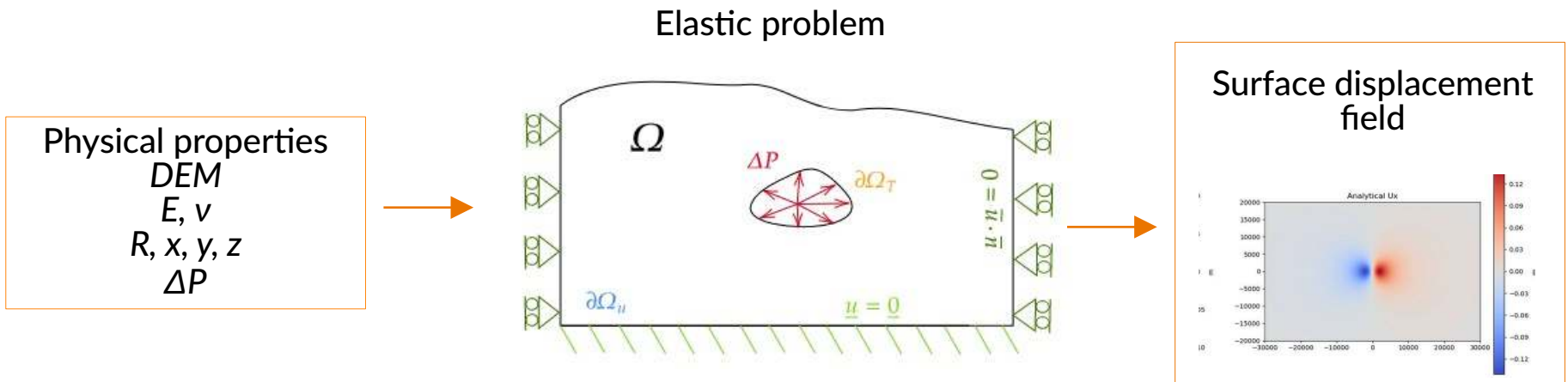
Other InSAR datasets after uniform  
downsampling (500 m steps)

=> Add information on displacement  
components

# Finite element based inversions - Forward models

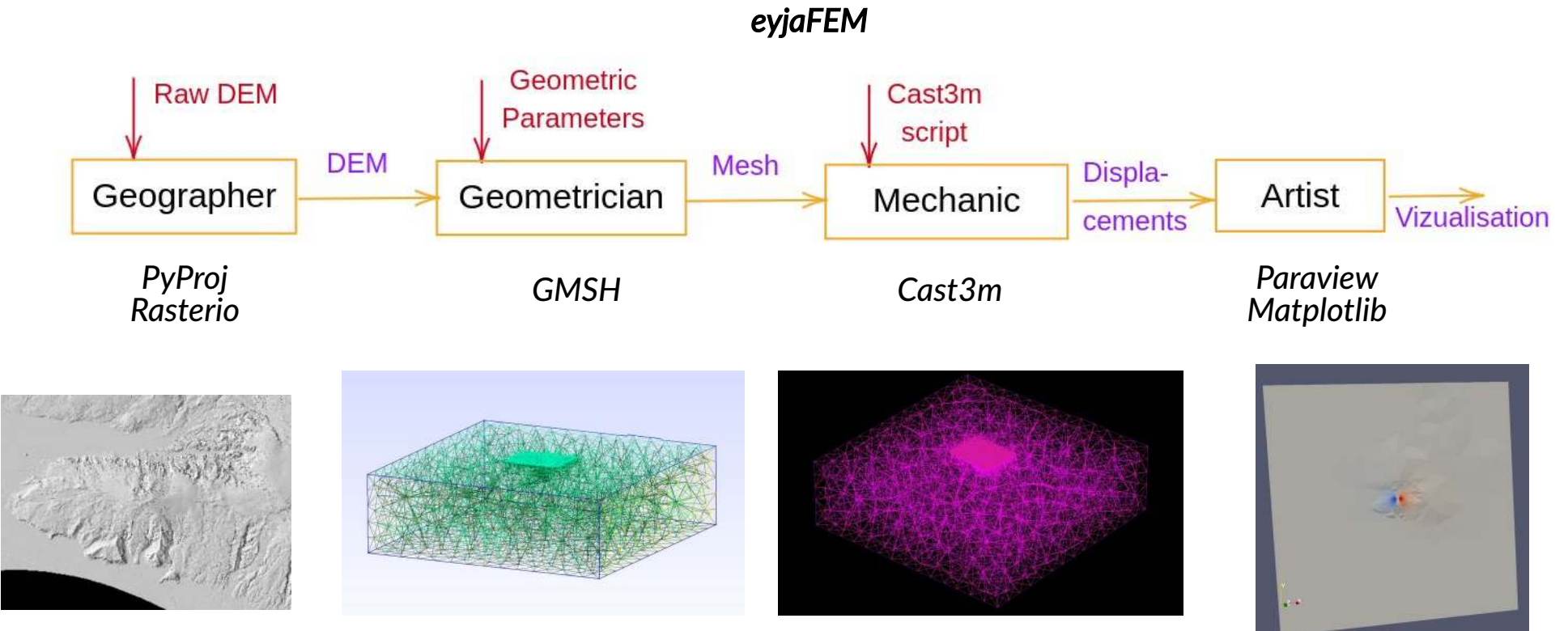
Objective : For a given source, get the surface displacement field

- Assumptions
  - Elastic, isotropic
  - No glacier or tectonic loading
  - Single pressure source
- Including
  - Spherical cavity uniformly pressurised
  - Topography



=>  $(x, y, z, \Delta P)$  are optimized ( $R$  fixed)

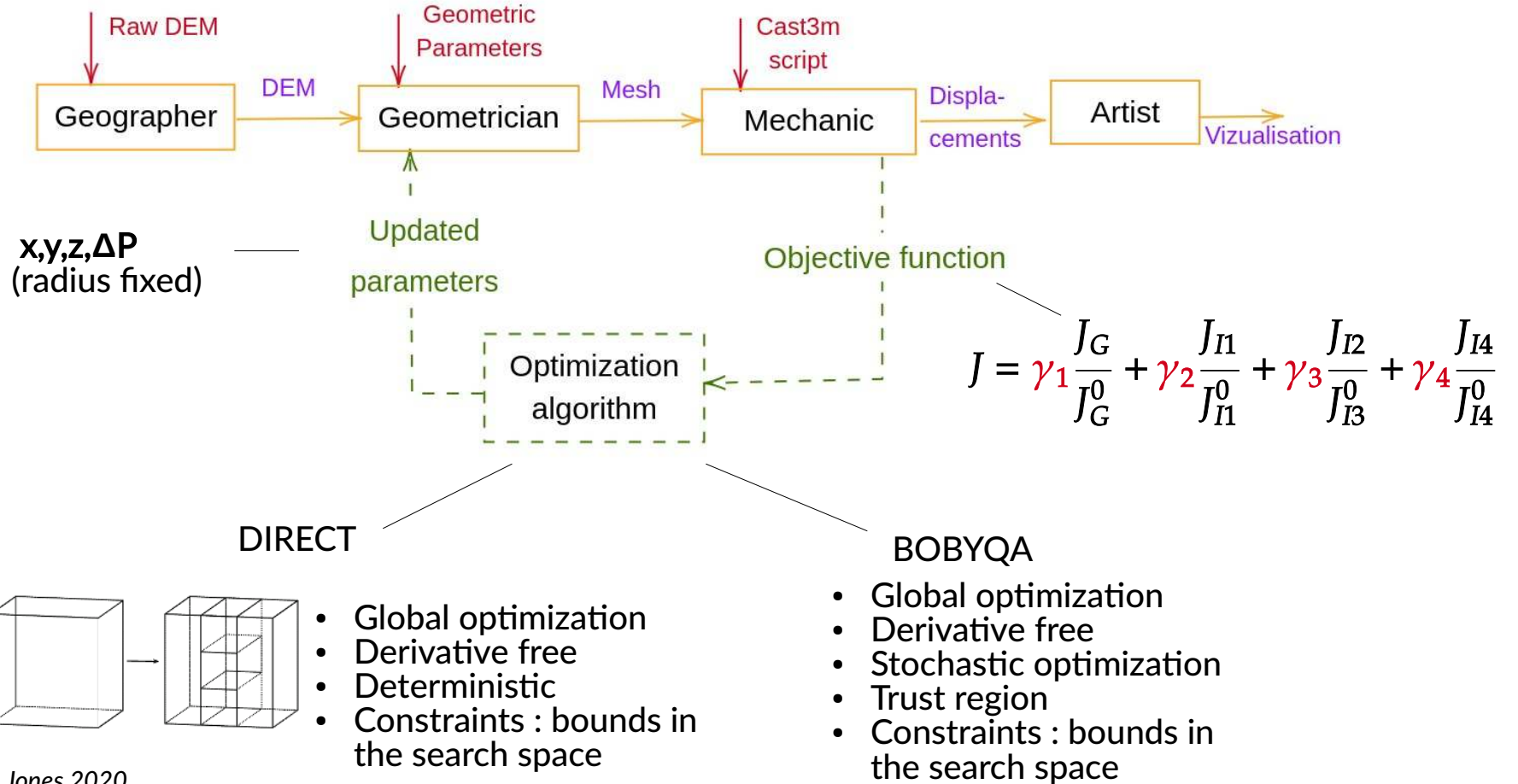
# Finite element based inversions - Software pipeline



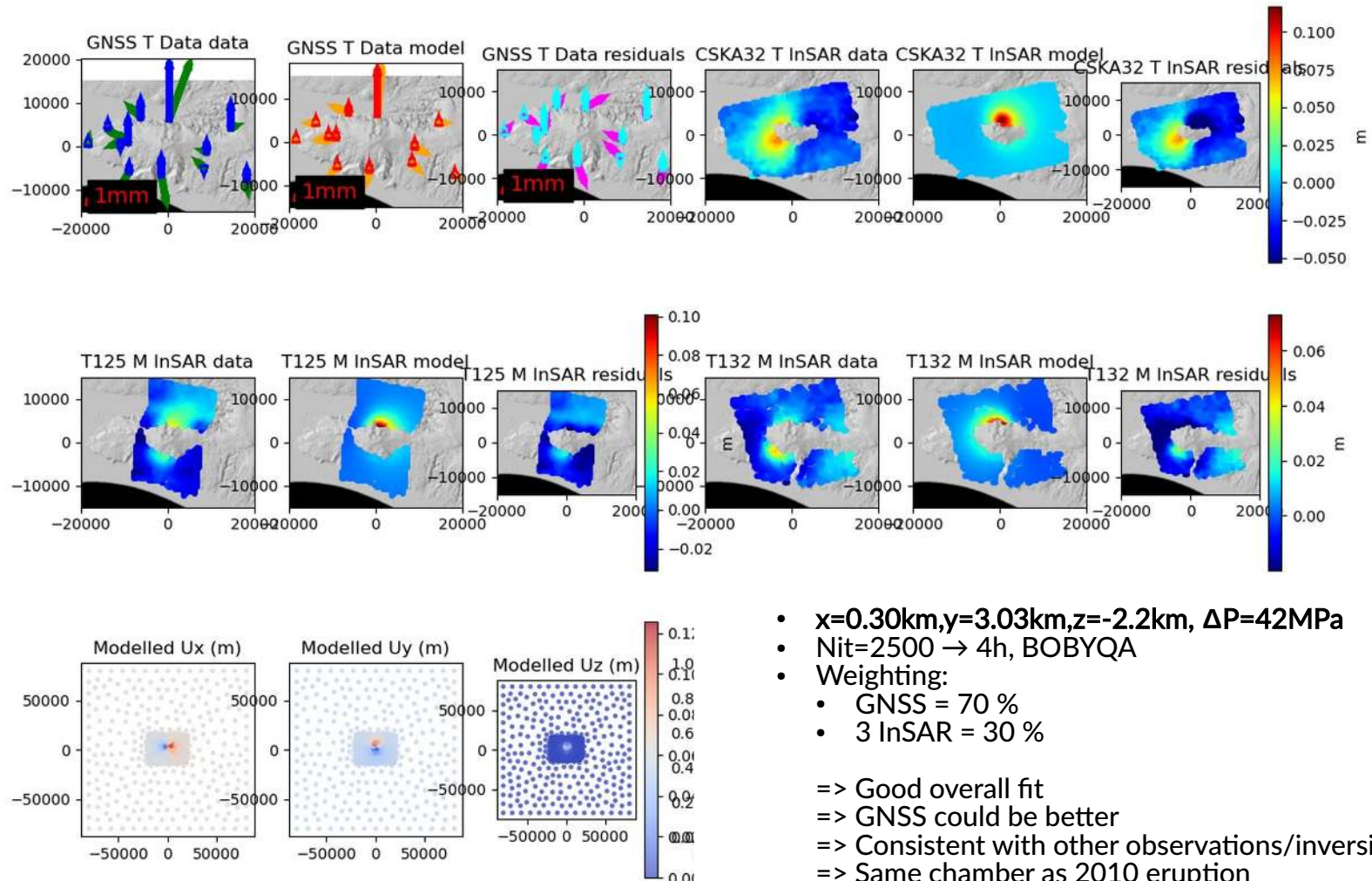
- Benchmarked against McTigue solution
- 2-3s for 1 full run

- Adaptable mesh size
- Can be extended to other problems

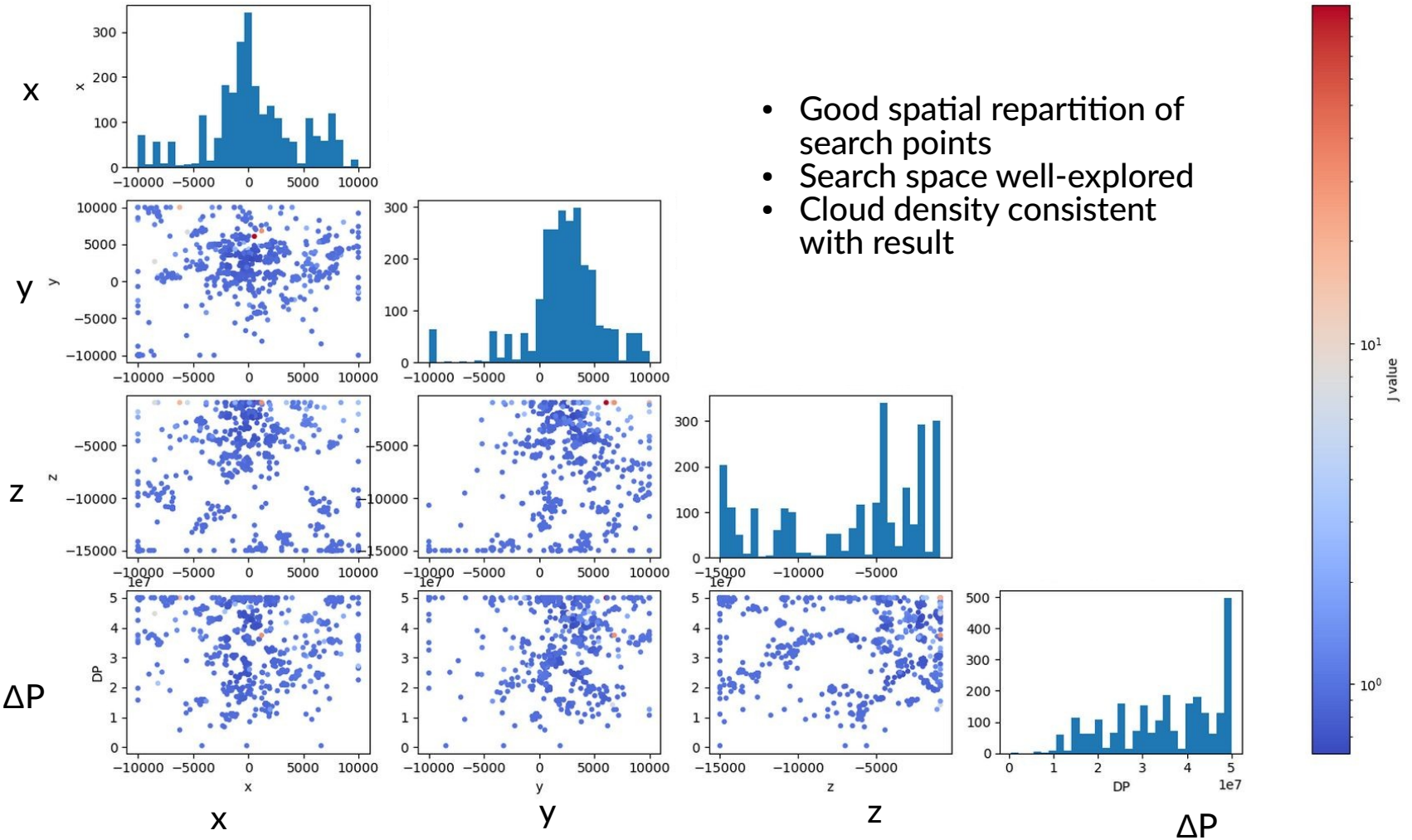
# Finite element based inversions - Optimization



# Results



# Results





## II

# Level-set shape optimization applied to magma domain inversion

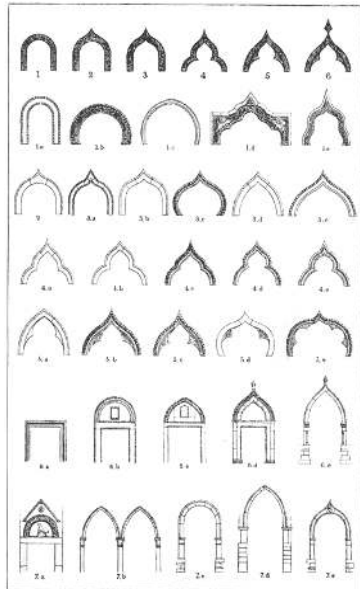
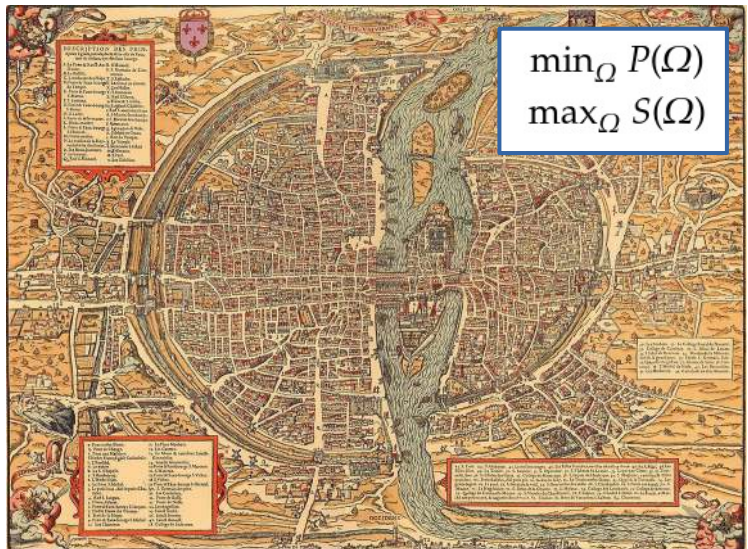


*Distant and close-up views  
of Bjartmanssteinn,  
Breiðafjörður*

# What is shape optimization ?

- Old question : What is the geometry that corresponds best to my problem ?

=> Formulation of an **optimization problem**  
(minimize/maximize a quantity)  
=> Non parametric

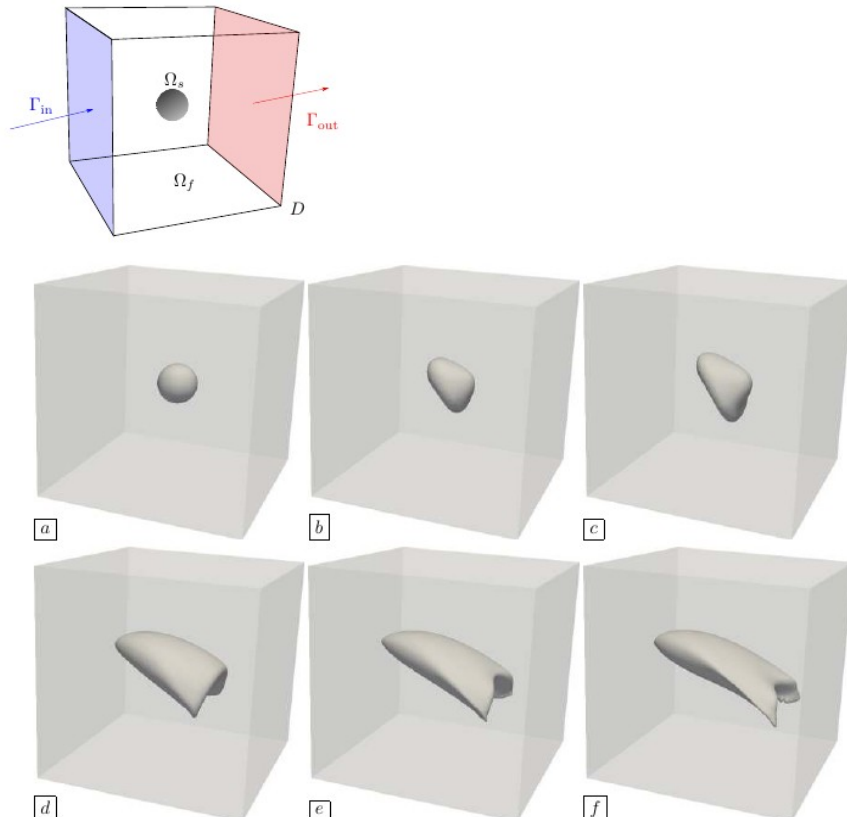


$\min_{\Omega} \vec{F}_x$

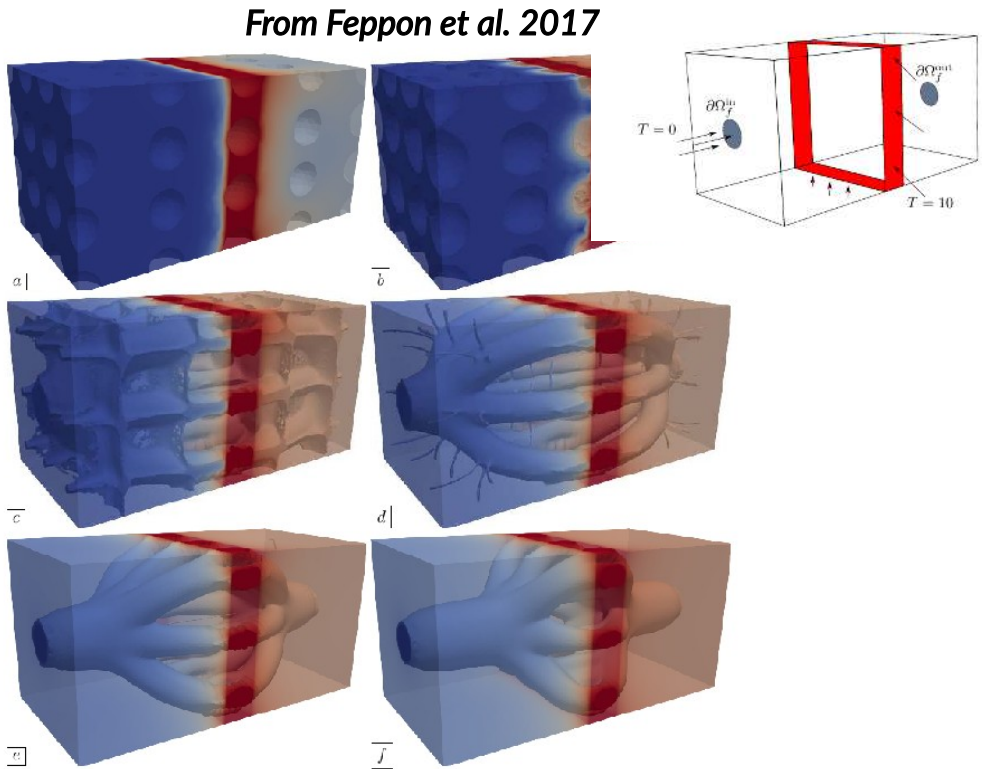


# What is shape optimization ?

Broad use in engineering, architecture ....



From Allair et al. 2018



COMSOL Blog

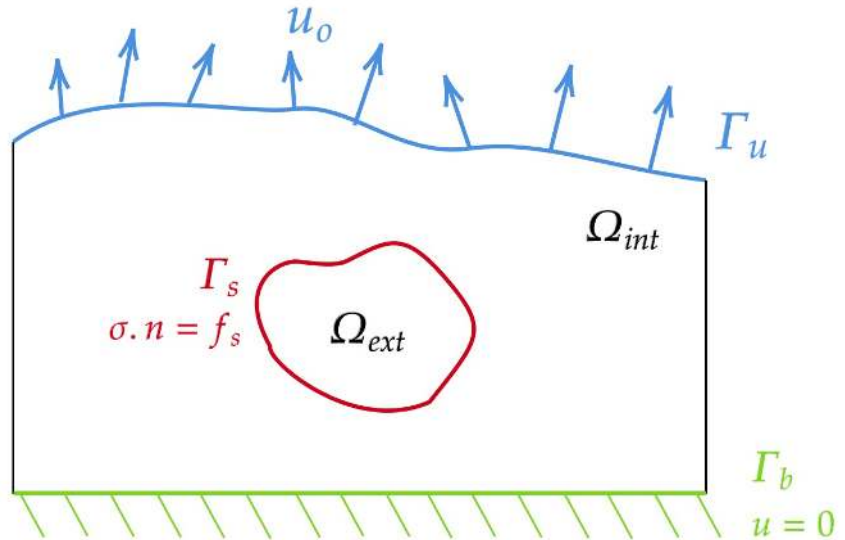
Designing New Structures with Shape Optimization

# Problem definition

## Find the best shape for a pressurized cavity

- Modelled surface displacement  $U$  from mechanical problem :
  - Domain  $\Omega = \Omega_{ext} \cup \Omega_{int}$
  - $\Omega_{int}$  = the magmatic body  
 $\rightarrow$  uniform pressure at the boundary :  $f_s = \Delta P \cdot n$   
 (Neumann), supposed **known**
  - Bottom surface is fixed (Dirichlet)
  - Surface displacement field  $U_o$  known on  $\Gamma_u$

=> Find  $\Omega_{ext}$  such  $U_o - U$  is min



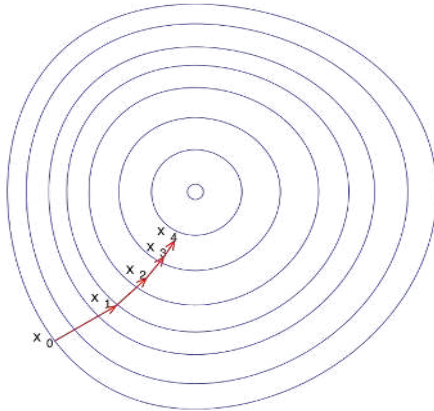
Governing equations

$$\begin{cases} -\operatorname{div}(Ae(u_\Omega)) = 0 & \text{in } \Omega, \\ u_\Omega = 0 & \text{on } \Gamma_D, \\ Ae(u_\Omega)n = g & \text{on } \Gamma_N, \\ Ae(u_\Omega)n = 0 & \text{on } \Gamma. \end{cases}$$

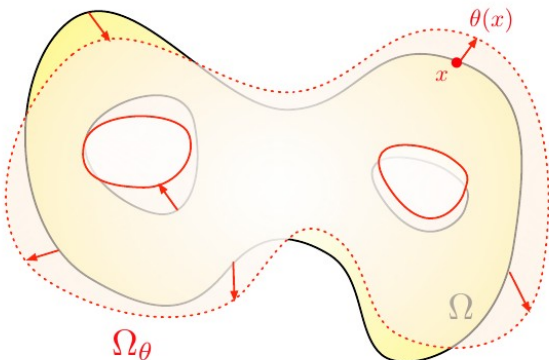
$$\min_{\Omega} J(\Omega) \Rightarrow J(\Omega) = \int_{\Gamma_u} (u(\Omega) - u_o)^2 dS$$

# Principle : shape derivative

- Gradient-based optimization of  $J$   
 At each step :
  - Compute  $\text{grad}(J(x))$
  - Find steepest descent direction  $\theta$
  - Move in the direction  $x + \theta$
=> Continue until no descent direction is available
- Can be stuck in local minima
- Needs an initialization (first) guess



$$J(\Omega_\theta) = J(\Omega) + J'(\Omega)(\theta)$$



From Dapogny et al. 2022

- Problem : what is the gradient of a shape ?
  - Derivation in respect to the shape
  - Direction  $\theta$
  - Small modification of the shape

$$J'(\Omega, \theta) = \int_{\Gamma_s} A e(u) : e(p). \theta. n dS + \int_{\Gamma_s} \left( \left( \frac{\partial f_s}{\partial n} p + \frac{\partial p}{\partial n} f_s \right) + \kappa f_s p \right) . \theta. n dS \quad ($$

=> Outputs  $\theta$ , steepest descent direction

# Principle : level-set method

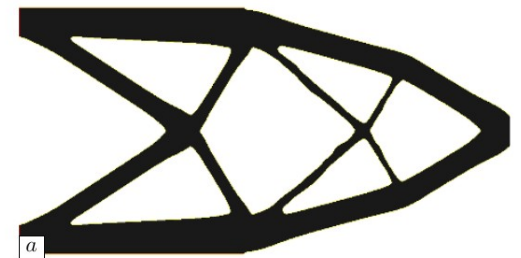
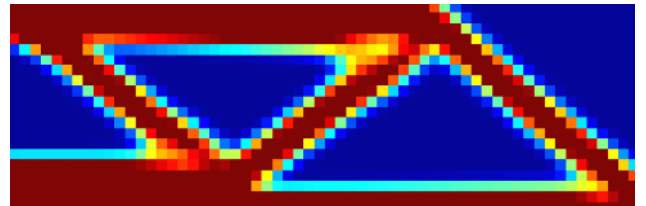
- Several methods exists
  - Density based
  - Level-set based
 => Better choice for the problem
- Level-set
  - Domain = slice of higher dimension smooth function
  - Allow use of description with PDE
 => Evolution defined with advection equation
- Practically, remeshed at each iteration

$$\frac{\partial \phi}{\partial t}(t, x) + v(t, x) \cdot \nabla \phi(t, x) = 0$$

Advection equation

Descent direction,  $v = -\tau^* \theta$

Density-based shape representation



From Dapogny et al. 2020

1.0E-11 1.0E-10 1.0E-09 1.0E-08 1.0E-07

2.0E-11 2.0E-10 2.0E-09 2.0E-08 2.0E-07

3.0E-11 3.0E-10 3.0E-09 3.0E-08 3.0E-07

4.0E-11 4.0E-10 4.0E-09 4.0E-08 4.0E-07

5.0E-11 5.0E-10 5.0E-09 5.0E-08 5.0E-07

6.0E-11 6.0E-10 6.0E-09 6.0E-08 6.0E-07

7.0E-11 7.0E-10 7.0E-09 7.0E-08 7.0E-07

8.0E-11 8.0E-10 8.0E-09 8.0E-08 8.0E-07

9.0E-11 9.0E-10 9.0E-09 9.0E-08 9.0E-07

1.0E-10 1.0E-09 1.0E-08 1.0E-07 1.0E-06

2.0E-10 2.0E-09 2.0E-08 2.0E-07 2.0E-06

3.0E-10 3.0E-09 3.0E-08 3.0E-07 3.0E-06

4.0E-10 4.0E-09 4.0E-08 4.0E-07 4.0E-06

5.0E-10 5.0E-09 5.0E-08 5.0E-07 5.0E-06

6.0E-10 6.0E-09 6.0E-08 6.0E-07 6.0E-06

7.0E-10 7.0E-09 7.0E-08 7.0E-07 7.0E-06

8.0E-10 8.0E-09 8.0E-08 8.0E-07 8.0E-06

9.0E-10 9.0E-09 9.0E-08 9.0E-07 9.0E-06

1.0E-09 1.0E-08 1.0E-07 1.0E-06 1.0E-05

2.0E-09 2.0E-08 2.0E-07 2.0E-06 2.0E-05

3.0E-09 3.0E-08 3.0E-07 3.0E-06 3.0E-05

4.0E-09 4.0E-08 4.0E-07 4.0E-06 4.0E-05

5.0E-09 5.0E-08 5.0E-07 5.0E-06 5.0E-05

6.0E-09 6.0E-08 6.0E-07 6.0E-06 6.0E-05

7.0E-09 7.0E-08 7.0E-07 7.0E-06 7.0E-05

8.0E-09 8.0E-08 8.0E-07 8.0E-06 8.0E-05

9.0E-09 9.0E-08 9.0E-07 9.0E-06 9.0E-05

1.0E-08 1.0E-07 1.0E-06 1.0E-05 1.0E-04

2.0E-08 2.0E-07 2.0E-06 2.0E-05 2.0E-04

3.0E-08 3.0E-07 3.0E-06 3.0E-05 3.0E-04

4.0E-08 4.0E-07 4.0E-06 4.0E-05 4.0E-04

5.0E-08 5.0E-07 5.0E-06 5.0E-05 5.0E-04

6.0E-08 6.0E-07 6.0E-06 6.0E-05 6.0E-04

7.0E-08 7.0E-07 7.0E-06 7.0E-05 7.0E-04

8.0E-08 8.0E-07 8.0E-06 8.0E-05 8.0E-04

9.0E-08 9.0E-07 9.0E-06 9.0E-05 9.0E-04

1.0E-07 1.0E-06 1.0E-05 1.0E-04 1.0E-03

2.0E-07 2.0E-06 2.0E-05 2.0E-04 2.0E-03

3.0E-07 3.0E-06 3.0E-05 3.0E-04 3.0E-03

4.0E-07 4.0E-06 4.0E-05 4.0E-04 4.0E-03

5.0E-07 5.0E-06 5.0E-05 5.0E-04 5.0E-03

6.0E-07 6.0E-06 6.0E-05 6.0E-04 6.0E-03

7.0E-07 7.0E-06 7.0E-05 7.0E-04 7.0E-03

8.0E-07 8.0E-06 8.0E-05 8.0E-04 8.0E-03

9.0E-07 9.0E-06 9.0E-05 9.0E-04 9.0E-03

1.0E-06 1.0E-05 1.0E-04 1.0E-03 1.0E-02

2.0E-06 2.0E-05 2.0E-04 2.0E-03 2.0E-02

3.0E-06 3.0E-05 3.0E-04 3.0E-03 3.0E-02

4.0E-06 4.0E-05 4.0E-04 4.0E-03 4.0E-02

5.0E-06 5.0E-05 5.0E-04 5.0E-03 5.0E-02

6.0E-06 6.0E-05 6.0E-04 6.0E-03 6.0E-02

7.0E-06 7.0E-05 7.0E-04 7.0E-03 7.0E-02

8.0E-06 8.0E-05 8.0E-04 8.0E-03 8.0E-02

9.0E-06 9.0E-05 9.0E-04 9.0E-03 9.0E-02

1.0E-05 1.0E-04 1.0E-03 1.0E-02 1.0E-01

2.0E-05 2.0E-04 2.0E-03 2.0E-02 2.0E-01

3.0E-05 3.0E-04 3.0E-03 3.0E-02 3.0E-01

4.0E-05 4.0E-04 4.0E-03 4.0E-02 4.0E-01

5.0E-05 5.0E-04 5.0E-03 5.0E-02 5.0E-01

6.0E-05 6.0E-04 6.0E-03 6.0E-02 6.0E-01

7.0E-05 7.0E-04 7.0E-03 7.0E-02 7.0E-01

8.0E-05 8.0E-04 8.0E-03 8.0E-02 8.0E-01

9.0E-05 9.0E-04 9.0E-03 9.0E-02 9.0E-01

1.0E-04 1.0E-03 1.0E-02 1.0E-01 1.0E+00

2.0E-04 2.0E-03 2.0E-02 2.0E-01 2.0E+00

3.0E-04 3.0E-03 3.0E-02 3.0E-01 3.0E+00

4.0E-04 4.0E-03 4.0E-02 4.0E-01 4.0E+00

5.0E-04 5.0E-03 5.0E-02 5.0E-01 5.0E+00

6.0E-04 6.0E-03 6.0E-02 6.0E-01 6.0E+00

7.0E-04 7.0E-03 7.0E-02 7.0E-01 7.0E+00

8.0E-04 8.0E-03 8.0E-02 8.0E-01 8.0E+00

9.0E-04 9.0E-03 9.0E-02 9.0E-01 9.0E+00

1.0E-03 1.0E-02 1.0E-01 1.0E+00 1.0E+01

2.0E-03 2.0E-02 2.0E-01 2.0E+00 2.0E+01

3.0E-03 3.0E-02 3.0E-01 3.0E+00 3.0E+01

4.0E-03 4.0E-02 4.0E-01 4.0E+00 4.0E+01

5.0E-03 5.0E-02 5.0E-01 5.0E+00 5.0E+01

6.0E-03 6.0E-02 6.0E-01 6.0E+00 6.0E+01

7.0E-03 7.0E-02 7.0E-01 7.0E+00 7.0E+01

8.0E-03 8.0E-02 8.0E-01 8.0E+00 8.0E+01

9.0E-03 9.0E-02 9.0E-01 9.0E+00 9.0E+01

1.0E-02 1.0E-01 1.0E+00 1.0E+01 1.0E+02

2.0E-02 2.0E-01 2.0E+00 2.0E+01 2.0E+02

3.0E-02 3.0E-01 3.0E+00 3.0E+01 3.0E+02

4.0E-02 4.0E-01 4.0E+00 4.0E+01 4.0E+02

5.0E-02 5.0E-01 5.0E+00 5.0E+01 5.0E+02

6.0E-02 6.0E-01 6.0E+00 6.0E+01 6.0E+02

7.0E-02 7.0E-01 7.0E+00 7.0E+01 7.0E+02

8.0E-02 8.0E-01 8.0E+00 8.0E+01 8.0E+02

9.0E-02 9.0E-01 9.0E+00 9.0E+01 9.0E+02

1.0E-01 1.0E+00 1.0E+01 1.0E+02 1.0E+03

2.0E-01 2.0E+00 2.0E+01 2.0E+02 2.0E+03

3.0E-01 3.0E+00 3.0E+01 3.0E+02 3.0E+03

4.0E-01 4.0E+00 4.0E+01 4.0E+02 4.0E+03

5.0E-01 5.0E+00 5.0E+01 5.0E+02 5.0E+03

6.0E-01 6.0E+00 6.0E+01 6.0E+02 6.0E+03

7.0E-01 7.0E+00 7.0E+01 7.0E+02 7.0E+03

8.0E-01 8.0E+00 8.0E+01 8.0E+02 8.0E+03

9.0E-01 9.0E+00 9.0E+01 9.0E+02 9.0E+03

1.0E+00 1.0E+01 1.0E+02 1.0E+03 1.0E+04

2.0E+00 2.0E+01 2.0E+02 2.0E+03 2.0E+04

3.0E+00 3.0E+01 3.0E+02 3.0E+03 3.0E+04

4.0E+00 4.0E+01 4.0E+02 4.0E+03 4.0E+04

5.0E+00 5.0E+01 5.0E+02 5.0E+03 5.0E+04

6.0E+00 6.0E+01 6.0E+02 6.0E+03 6.0E+04

7.0E+00 7.0E+01 7.0E+02 7.0E+03 7.0E+04

8.0E+00 8.0E+01 8.0E+02 8.0E+03 8.0E+04

9.0E+00 9.0E+01 9.0E+02 9.0E+03 9.0E+04

1.0E+01 1.0E+02 1.0E+03 1.0E+04 1.0E+05

2.0E+01 2.0E+02 2.0E+03 2.0E+04 2.0E+05

3.0E+01 3.0E+02 3.0E+03 3.0E+04 3.0E+05

4.0E+01 4.0E+02 4.0E+03 4.0E+04 4.0E+05

5.0E+01 5.0E+02 5.0E+03 5.0E+04 5.0E+05

6.0E+01 6.0E+02 6.0E+03 6.0E+04 6.0E+05

7.0E+01 7.0E+02 7.0E+03 7.0E+04 7.0E+05

8.0E+01 8.0E+02 8.0E+03 8.0E+04 8.0E+05

9.0E+01 9.0E+02 9.0E+03 9.0E+04 9.0E+05

1.0E+02 1.0E+03 1.0E+04 1.0E+05 1.0E+06

2.0E+02 2.0E+03 2.0E+04 2.0E+05 2.0E+06

3.0E+02 3.0E+03 3.0E+04 3.0E+05 3.0E+06

4.0E+02 4.0E+03 4.0E+04 4.0E+05 4.0E+06

5.0E+02 5.0E+03 5.0E+04 5.0E+05 5.0E+06

6.0E+02 6.0E+03 6.0E+04 6.0E+05 6.0E+06

7.0E+02 7.0E+03 7.0E+04 7.0E+05 7.0E+06

8.0E+02 8.0E+03 8.0E+04 8.0E+05 8.0E+06

9.0E+02 9.0E+03 9.0E+04 9.0E+05 9.0E+06

1.0E+03 1.0E+04 1.0E+05 1.0E+06 1.0E+07

2.0E+03 2.0E+04 2.0E+05 2.0E+06 2.0E+07

3.0E+03 3.0E+04 3.0E+05 3.0E+06 3.0E+07

4.0E+03 4.0E+04 4.0E+05 4.0E+06 4.0E+07

5.0E+03 5.0E+04 5.0E+05 5.0E+06 5.0E+07

6.0E+03 6.0E+04 6.0E+05 6.0E+06 6.0E+07

7.0E+03 7.0E+04 7.0E+05 7.0E+06 7.0E+07

8.0E+03 8.0E+04 8.0E+05 8.0E+06 8.0E+07

9.0E+03 9.0E+04 9.0E+05 9.0E+06 9.0E+07

1.0E+04 1.0E+05 1.0E+06 1.0E+07 1.0E+08

2.0E+04 2.0E+05 2.0E+06 2.0E+07 2.0E+08

3.0E+04 3.0E+05 3.0E+06 3.0E+07 3.0E+08

4.0E+04 4.0E+05 4.0E+06 4.0E+07 4.0E+08

5.0E+04 5.0E+05 5.0E+06 5.0E+07 5.0E+08

6.0E+04 6.0E+05 6.0E+06 6.0E+07 6.0E+08

7.0E+04 7.0E+05 7.0E+06 7.0E+07 7.0E+08

8.0E+04 8.0E+05 8.0E+06 8.0E+07 8.0E+08

9.0E+04 9.0E+05 9.0E+06 9.0E+07 9.0E+08

1.0E+05 1.0E+06 1.0E+07 1.0E+08 1.0E+09

2.0E+05 2.0E+06 2.0E+07 2.0E+08 2.0E+09

3.0E+05 3.0E+06 3.0E+07 3.0E+08 3.0E+09

4.0E+05 4.0E+06 4.0E+07 4.0E+08 4.0E+09

5.0E+05 5.0E+06 5.0E+07 5.0E+08 5.0E+09

6.0E+05 6.0E+06 6.0E+07 6.0E+08 6.0E+09

7.0E+05 7.0E+06 7.0E+07 7.0E+08 7.0E+09

8.0E+05 8.0E+06 8.0E+07 8.0E+08 8.0E+09

9.0E+05 9.0E+06 9.0E+07 9.0E+08 9.0E+09

1.0E+06 1.0E+07 1.0E+08 1.0E+09 1.0E+10

2.0E+06 2.0E+07 2.0E+08 2.0E+09 2.0E+10

3.0E+06 3.0E+07 3.0E+08 3.0E+09 3.0E+10

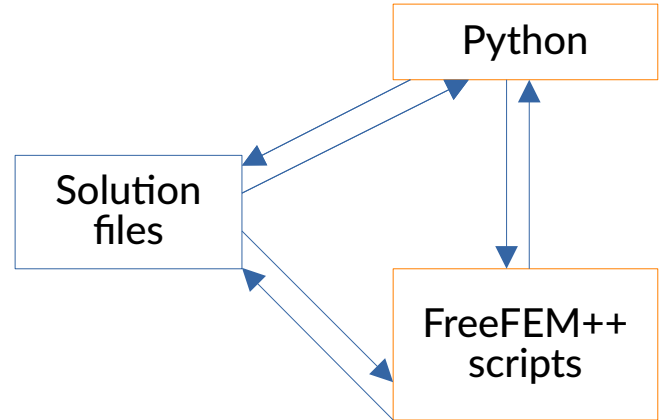
4.0E+06 4.0E+07 4.0E+08 4.0E+09 4.0E+10

5.0E+06 5.0E+07 5.0E+08 5.0E+09 5.0E+10

# Implementation:sotuto

---

- Sotuto
  - Python-Freefem implementation of shape optimization
  - Freefem
    - Finite element software based on variational formulation




---

**Algorithm 1** Generic shape gradient algorithm.

---

**Initialization:** Initial shape  $\Omega^0$ .  
**for**  $n = 0, \dots$ , until convergence **do**

- (1) Calculate the solution  $u_{\Omega^n}$  (resp.  $p_{\Omega^n}$ ) to the state (resp. adjoint) equation posed in  $\Omega^n$ .
- (2) From the theoretical formulas for the shape derivatives  $J'(\Omega)(\theta)$ ,  $G'(\Omega)(\theta)$  and  $H'(\Omega)(\theta)$ , infer a descent direction  $\theta^n$  from  $\Omega^n$  for the shape optimization problem (2.2).
- (3) Deform  $\Omega^n$  according to  $\theta^n$  for a small descent step  $\tau^n > 0$ , so that the new shape

$$\Omega^{n+1} := (\text{Id} + \tau^n \theta^n)(\Omega^n)$$

is “better” than the previous one in view of (2.2).

**end for**

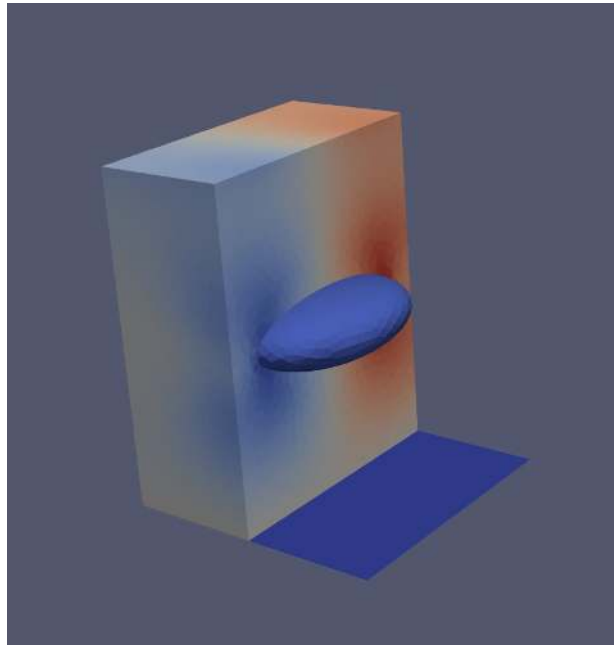
**return**  $\Omega^n$

---

3 fem  
resolution

# Method benchmarking

- Initial guess : ellipsoid
- Input synthetic displacement field of a sphere
- Test convergence and robustness : will it find a sphere ?



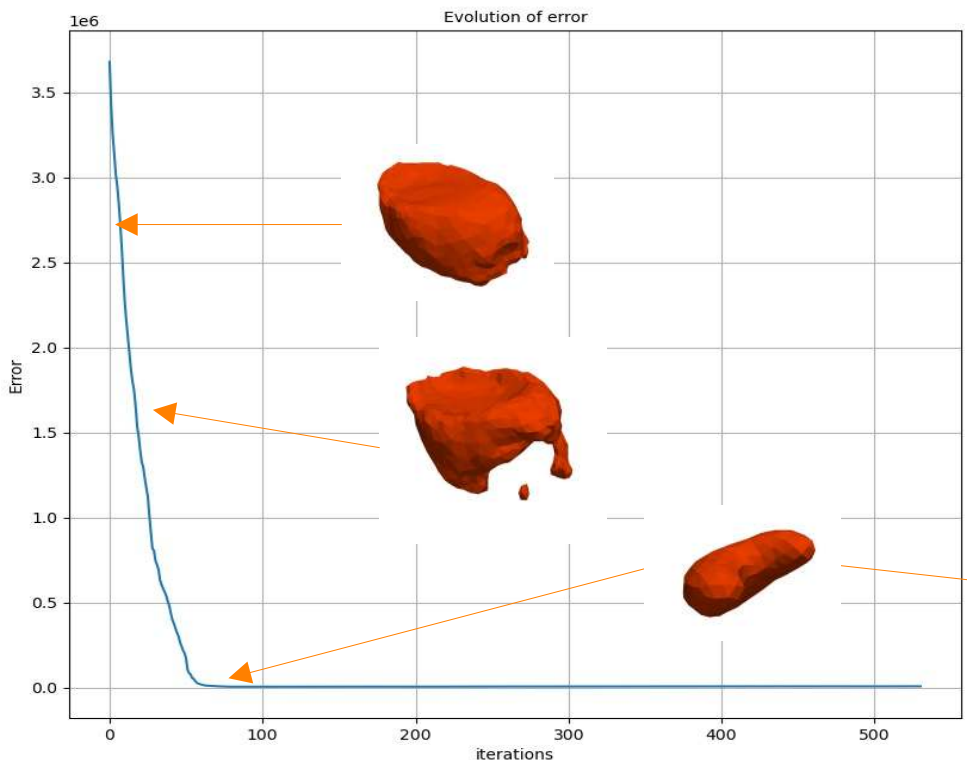
## Algorithm parameters

```

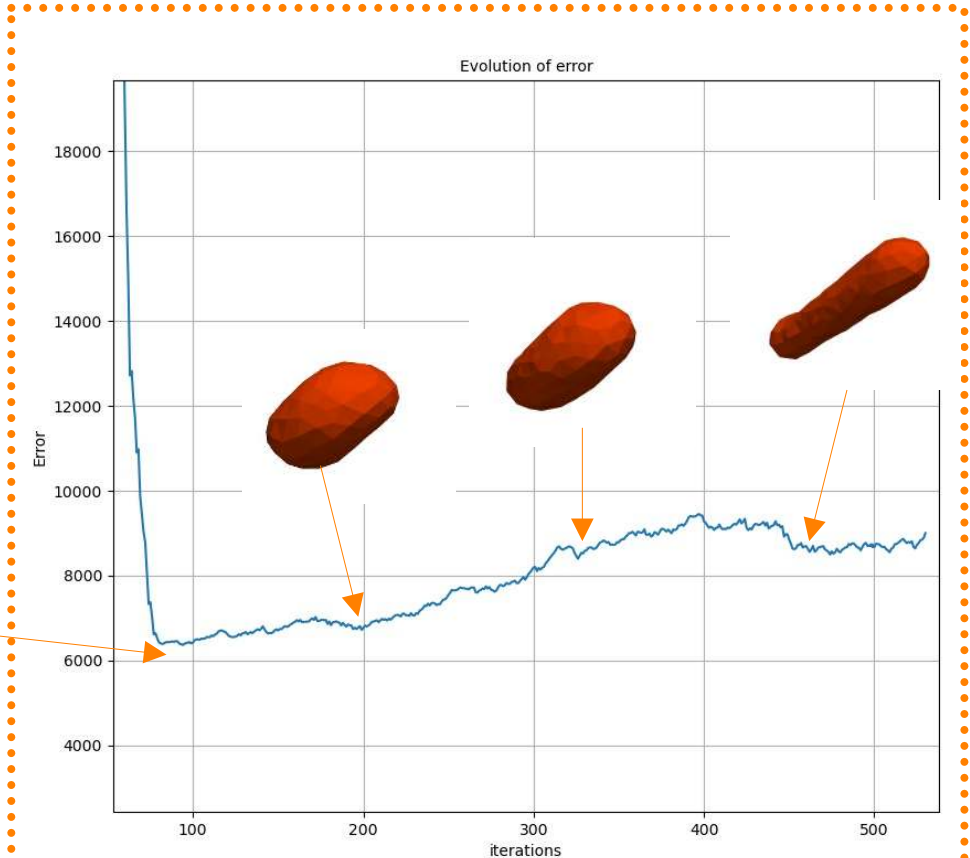
16 # Magmatic source problem parameters
17 YOUNG = 30e9 ; #E
18 POISS = 0.25 ; #nu
19 PRESS = 10e6 ; #Pressure change DP (source load)
20 DEPTH = 5e3 ; #depth of source
21 RVRAI = 1e3 ; # radius of the target analytical spherical source
22 REX = 2e3 #semi axes of intial ellipsoidal source
23 REY = 3e3
24 REZ = 1e3
25 # REX = RVRAI ; REY = REX ; REZ = REX ; #FOR TESTING
26
27 # Parameters of the mesh
28 MESHIZ = 300
29 HMIN = 200 #minimu autorized element lenght
30 HMAX = 700 #maximum authorized element length
31 HAUSD = 50 #mawimum authorized gap between ideal shape and its mesh nodes
32 HGRAD = 1.4 #max rati allowed between 2 adjascent edges
33 XEXT = 8e3 #extent of domain in X direction
34 YEXT = 8e3 #extent of domain in X direction
35 ZEXT = 10e3 #extent of domain in X direction
36
37 # Other parameters
38 EPS = 1e-10 # Precision parameter
39 EPSP = 1e-20 # Precision parameter for packing
40 ALPHA = 50 # Parameter for velocity extension - regularization
41 ALPHALS = 10 # Parameter for regularization of LS function
42 MAXIT = 2000 # Maximum number of iterations in the shape optimization proce
43 MAXITLS = 10 # Maximum number of iterations in the line search procedure
44 MAXCOEF = 3 # Maximum allowed move between two iterations (in # * MESHIZ)
45 MINCOEF = 0.02 # Minimum allowed move between two iterations (in # * MESHIZ)
46 TOL = 0.01 # Tolerance for a slight increase in the merit
47 AJ = 1.0 # Weight of objective in null-space optimization algorithm
48 AG = 0.0 # Weight of constraint in null-space optimization algorithm
49 ITMAXNORMXIJ = 200
50 ERRTOL = 5e3 #tolerance for slight error increase
51 ERRMOD = 0

```

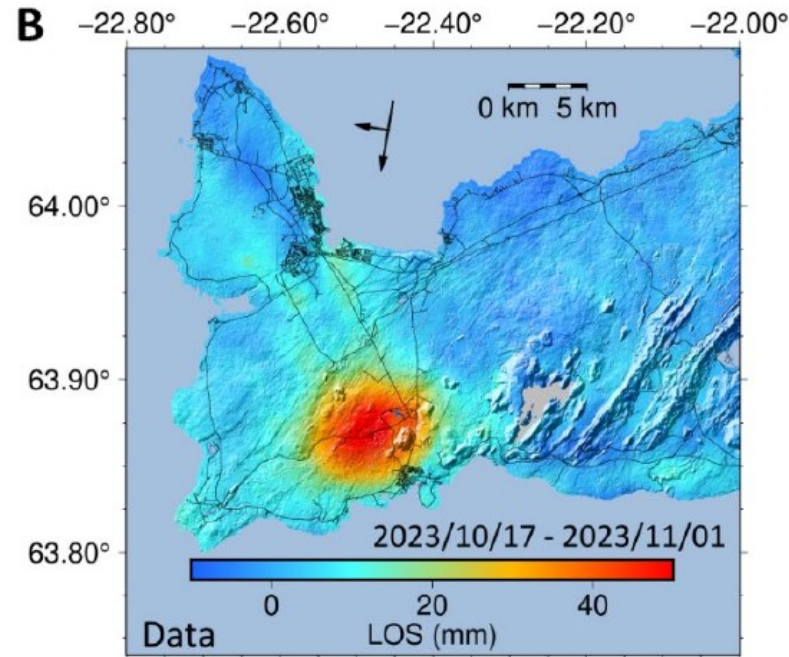
# Results



- Good degrowth:  $N_{min}=86$
- Total time  $\sim 1h30$
- Best shape is sphere like
  - Mesh size
  - Domain size



## Test on real data



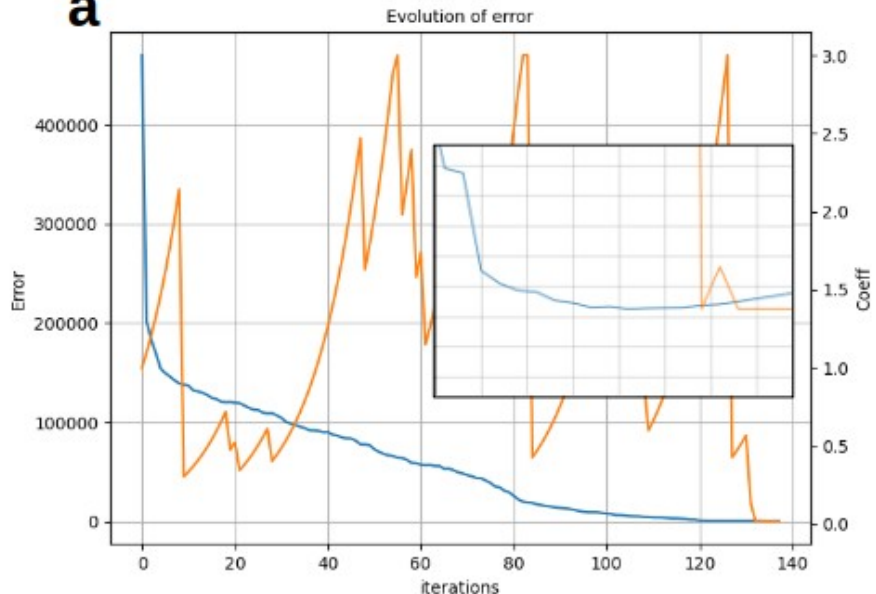
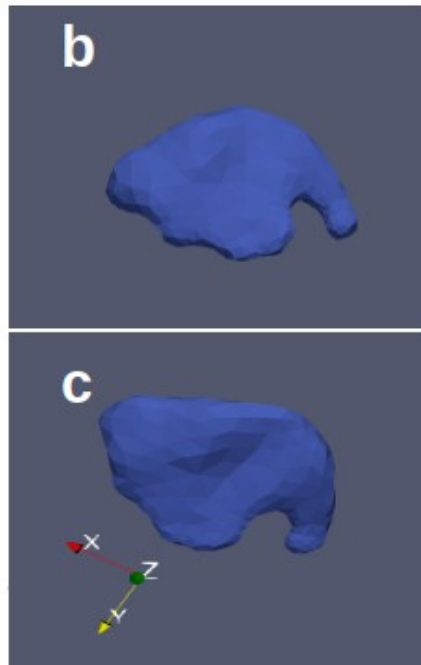
From Sigmundsson et al. 2024

- Recharge of deep reservoir
- 21 April-14 June 2024
- 2 InSAR tracks

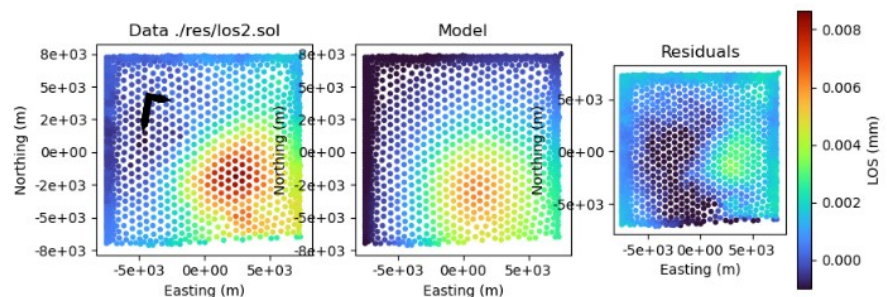
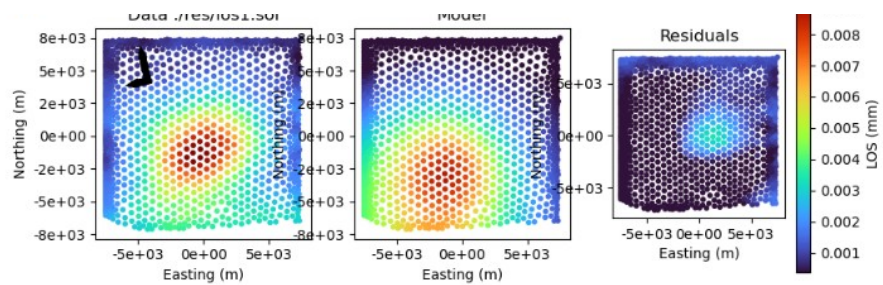


Eruption of 3 August 2024, Meradalir

# Test on real data

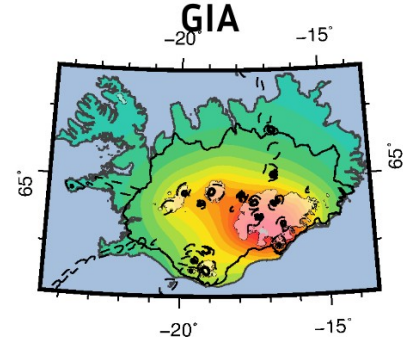
**a****b****c**

- Good matching of the data
- Different convergence pattern ( $J$  influence?)
- Shape consistent with other observation/inversions
- Horn and other features artifacts ?

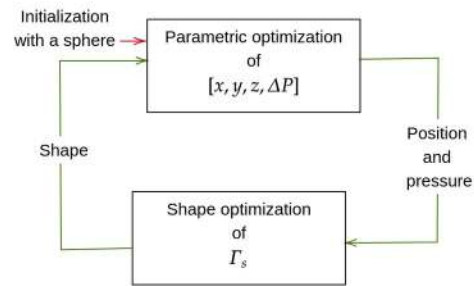


# General conclusion

- More exploration of algorithms is needed (convergence, weighting, control parameters)
  - Optimize computation efficiency (parallel computing)
  - Complexity can be added
    - Visco-elasticity, poro-elasticity
    - Glacier melting influence => ISVOLC
    - Additional loadings (glacier, tectonics, tides)
    - Heterogeneities
  - Embedded shape optimization loop in global optimization
  - Global parametrized optimization of 2011-2015 inflation (I)
    - Rely on derivatives of  $J$
    - Study potential 2015 dike intrusion
    - Quantify uncertainties
  - Shape optimization (II)
    - Influence of data distribution
    - Influence of initial guess
    - Rigorous study of underdetermination effects
- Overall may help in magmatic source inversion for hazard assessment



Drouin 2018



Sigmundsson 2024

# References - I

1. Adalgeirsdóttir, G. et al. Glacier Changes in Iceland From ~1890 to 2019. *Front. Earth Sci.* 8, (2020).
2. Albino, F. & Sigmundsson, F. Stress transfer between magma bodies: Influence of intrusions prior to 2010 eruptions at Eyjafjallajökull volcano, Iceland. *Journal of Geophysical Research: Solid Earth* 119, 2964–2975 (2014).
3. Alshembari, R., Hickey, J., Williamson, B. J. & Cashman, K. Poroelastic Mechanical Behavior of Crystal Mush Reservoirs: Insights Into the Spatio-Temporal Evolution of Volcano Surface Deformation. *Journal of Geophysical Research: Solid Earth* 127, e2022JB024332 (2022).
4. Altamimi, Z., Rebischung, P., Métivier, L. & Collilieux, X. ITRF2014: A new release of the International Terrestrial Reference Frame modeling nonlinear station motions. *JGR Solid Earth* 121, 6109–6131 (2016).
5. Bagnardi, M. & Hooper, A. Inversion of Surface Deformation Data for Rapid Estimates of Source Parameters and Uncertainties: A Bayesian Approach. *Geochem Geophys Geosyst* 19, 2194–2211 (2018).
6. Belart, J. M. C. et al. The geodetic mass balance of Eyjafjallajökull ice cap for 1945–2014: processing guidelines and relation to climate. *J. Glaciol.* 65, 395–409 (2019).
7. Cartis, C., Roberts, L. & Sheridan-Methven, O. Escaping local minima with local derivative-free methods: a numerical investigation. *Optimization* 71, 2343–2373 (2022).
8. Dapogny, C. & Feppon, F. Shape optimization using a level set based mesh evolution method: an overview and tutorial. *Comptes Rendus. Mathématique* 361, 1267–1332 (2023).
9. Del Negro, C., Currenti, G. & Scandura, D. Temperature-dependent viscoelastic modeling of ground deformation: Application to Etna volcano during the 1993–1997 inflation period. *Physics of the Earth and Planetary Interiors* 172, 299–309 (2009).
10. Drouin, V., Heki, K., Sigmundsson, F., Hreinsdóttir, S. & Ófeigsson, B. G. Constraints on seasonal load variations and regional rigidity from continuous GPS measurements in Iceland, 1997–2014. *Geophys. J. Int.* 205, 1843–1858 (2016).
11. Drouin, V. & Sigmundsson, F. Countrywide Observations of Plate Spreading and Glacial Isostatic Adjustment in Iceland Inferred by Sentinel-1 Radar Interferometry, 2015–2018. *Geophysical Research Letters* 46, 8046–8055 (2019).
12. Dzurisin, D. *Volcano Deformation: Geodetic Monitoring Techniques*. (Springer ; Praxis, Berlin ; New York : Chichester, UK, 2007).
13. Fialko, Y., Khazan, Y. & Simons, M. Deformation due to a pressurized horizontal circular crack in an elastic half-space, with applications to volcano geodesy. *Geophysical Journal International* 146, 181–190 (2001).
14. Fletcher, K. *InSAR Principles: Guidelines for SAR Interferometry Processing and Interpretation*. (ESA Publications Division, ESTEC, Noordwijk, the Netherlands, 2007).
15. Floyd, M. *GAMIT/GLOBK Documentation*. GAMIT/GLOBK Documentation <http://geoweb.mit.edu/gg/docs.php>.
16. Geuzaine, C. *Gmsh Manual 4.13.1*. <https://gmsh.info/doc/texinfo/gmsh.html>.
17. Geuzaine, C., Remacle, J.-F. & Dular, P. Gmsh: a three-dimensional finite element mesh generator. *International Journal for Numerical Methods in Engineering* 79, 1309–1331 (2009).
18. Greiner, S. H. Including topography and a 3D-elastic structure into a Finite-Element deformation model of Grímsvötn, Iceland. (2021).
19. Grémion, S. Eyjafjallajökull ground deformation history between 2009 and 2019 using InSAR timeseries and magma sources modelling. (University of Iceland, 2020).
20. Guðmundsson, M. T. & Höskuldsson, Á. Icelandic Volcanoes. <https://icelandicvolcanos.is/?volcano=EYJ> (2019).
21. Guglielmino, F., Nunnari, G., Puglisi, G. & Spata, A. Simultaneous and Integrated Strain Tensor Estimation From Geodetic and Satellite Deformation Measurements to Obtain Three-Dimensional Displacement Maps. *IEEE Trans. Geosci. Remote Sensing* 49, 1815–1826 (2011).
22. Hecht, F. New development in FreeFem++. *J. Numer. Math.* 20, 251–265 (2012).
23. Hickey, J. & Gottsmann, J. Benchmarking and developing numerical Finite Element models of volcanic deformation. *Journal of Volcanology and Geothermal Research* 280, 126–130 (2014).
24. Hooper, A., Segall, P. & Zebker, H. Persistent scatterer interferometric synthetic aperture radar for crustal deformation analysis, with application to Volcán Alcedo, Galápagos. *J. Geophys. Res.* 112, 2006JB004763 (2007).
25. Hooper, A., Bekaert, D., Spaans, K. & Arikan, M. Recent advances in SAR interferometry time series analysis for measuring crustal deformation. *Tectonophysics* 514–517, 1–13 (2012).

26. Jones, D. R., Perttunen, C. D. & Stuckman, B. E. Lipschitzian optimization without the Lipschitz constant. *J Optim Theory Appl* 79, 157–181 (1993).
27. Jones, D. R. & Martins, J. R. R. A. The DIRECT algorithm: 25 years Later. *J Glob Optim* 79, 521–566 (2021).
28. Kampes, B. & Usai, S. Doris: the Delft Object-oriented Radar Interferometric Software. in (Enschede, The Netherlands, 1999).
29. La Borderie, C. Cast3M, a multi-physic finite element program opened to the research community. in Heat, light and wind simulation on an urban scale (Anglet, France, 2017).
30. McTigue, D. F. Elastic stress and deformation near a finite spherical magma body: Resolution of the point source paradox. *J. Geophys. Res.* 92, 12931–12940 (1987).
31. Menke, W. *Geophysical Data Analysis: Discrete Inverse Theory*. (Academic Press, Waltham, MA, 2012).
32. Mogi, K. Relations between the eruptions of various volcanoes and the deformations of the ground surfaces around them. *Earthq Res Inst* 36, 99–134 (1958).
33. O'Hara, C. Estimating deformation source parameters using a 3D elastic finite element model including topography and crustal heterogeneity at Askja, Iceland. (2023).
34. Okada, Y. Surface deformation due to shear and tensile faults in a half-space. *Bulletin of the Seismological Society of America* 75, 1135–1154 (1985).
35. Parks, M. & ISVOLC Team. An update of recent geodetic observations and modelling results at key Icelandic volcanoes within the ISVOLC project. <https://meetingorganizer.copernicus.org/EGU24/EGU24-19525.html> (2024) doi:10.5194/egusphere-egu24-19525.
36. Parks, M. M. et al. 2021–2023 Unrest and Geodetic Observations at Askja Volcano, Iceland. *Geophysical Research Letters* 51, e2023GL106730 (2024).
37. Powell, M. The BOBYQA Algorithm for Bound Constrained Optimization without Derivatives. Technical Report, Department of Applied Mathematics and Theoretical Physics (2009).
38. Rios, L. M. & Sahinidis, N. V. Derivative-free optimization: a review of algorithms and comparison of software implementations. *J Glob Optim* 56, 1247–1293 (2013).
39. Schmidt, P., Lund, B., Hieronymus, C. & Näslund, J.-O. 3D GIA-modelling of northern Europe with varying lithospheric thickness. 8802 (2010).
40. Segall, P. *Earthquake and Volcano Deformation*. (Princeton university press, Princeton, N. J, 2010).
41. Segall, P. Magma chambers: what we can, and cannot, learn from volcano geodesy. *Philosophical Transactions of the Royal Society A: Mathematical, Physical and Engineering Sciences* 377, 20180158 (2019).
42. Shahriari, B., Swersky, K., Wang, Z., Adams, R. P. & de Freitas, N. Taking the Human Out of the Loop: A Review of Bayesian Optimization. *Proceedings of the IEEE* 104, 148–175 (2016).
43. Sigmundsson, F. *Iceland Geodynamics: Crustal Deformation and Divergent Plate Tectonics*. (Springer ; In association with Praxis Pub, Berlin ; New York : Chichester, UK, 2006).
44. Sigmundsson, F. et al. Geodynamics of Iceland and the signatures of plate spreading. *Journal of Volcanology and Geothermal Research* 391, 106436 (2020).
45. Sigmundsson, F. et al. Intrusion triggering of the 2010 Eyjafjallajökull explosive eruption. *Nature* 468, 426–430 (2010).
46. Sigmundsson, F. et al. Chapter 15 - Influence of climate change on magmatic processes: What does geodesy and modeling of geodetic data tell us? in *GNSS Monitoring of the Terrestrial Environment* (eds. Aoki, Y. & Kreemer, C.) 287–299 (Elsevier, 2024). doi:10.1016/B978-0-323-95507-2.00013-X.
47. Sigmundsson, F. et al. Fracturing and tectonic stress drives ultrarapid magma flow into dikes. *Science* eadn2838 (2024) doi:10.1126/science.adn2838.
48. Sigmundsson, F. et al. Chapter 11 - Magma Movements in Volcanic Plumbing Systems and their Associated Ground Deformation and Seismic Patterns. in *Volcanic and Igneous Plumbing Systems* (ed. Burchardt, S.) 285–322 (Elsevier, 2018). doi:10.1016/B978-0-12-809749-6.00011-X.
49. Sigurðardóttir, F. M. Modelling of ground deformation at Eyjafjallajökull volcano 2011–2015. (Faculty of Earth Sciences, University of Iceland, Reykjavik, 2024).
50. Spaans, K., Hreinsdóttir, S., Hooper, A. & Ófeigsson, B. G. Crustal movements due to Iceland's shrinking ice caps mimic magma inflow signal at Katla volcano. *Sci Rep* 5, 10285 (2015).
51. UNAVCO. Plate Motion Calculator. <https://www.unavco.org/software/geodetic-utilities/plate-motion-calculator/plate-motion-calculator.html#usage>.
52. Valsson, G. Þ. ISN2016 - Tækniþýrsla. <https://www.lmi.is/is/um-lmi/frettafyrilit/isn2016-tkniskrsla> (2019).
53. Van Stein, B., Wang, H., Kowalczyk, W. & Bäck, T. A Novel Uncertainty Quantification Method for Efficient Global Optimization. in *Information Processing and Management of Uncertainty in Knowledge-Based Systems. Applications* (eds. Medina, J. et al.) vol. 855 480–491 (Springer International Publishing, Cham, 2018).
54. Virtanen, P. et al. SciPy 1.0: fundamental algorithms for scientific computing in Python. *Nat Methods* 17, 261–272 (2020).
55. Xiang, Y. & Gong, X. G. Efficiency of generalized simulated annealing. *Phys. Rev. E* 62, 4473–4476 (2000).
56. Yang, Y., Sigmundsson, F. & Geirsson, H. Joint Bayesian Modeling of Velocity Break Points, Noise Characteristics, and Their Uncertainties in GNSS Time Series: Far-Field Velocity Anomalies Concurrent With Magmatic Activity in Iceland. *Geophysical Research Letters* 50, e2023GL103432 (2023).

# References - II

1. Allaire, G. *Conception optimale de structures*. vol. 58 (Springer Berlin Heidelberg, 2006).
2. Allaire, G., Dapogny, C. & Jouve, F. Chapter 1 - Shape and topology optimization. in *Geometric partial differential equations - part II* (eds. Bonito, A. & Nochetto, R. H.) vol. 22 1-132 (Elsevier, 2021).
3. Andreassen, E., Clausen, A., Schevenels, M., Lazarov, B. S. & Sigmund, O. Efficient topology optimization in MATLAB using 88 lines of code. *Struct Multidisc Optim* 43, 1-16 (2011).
4. Bagnardi, M. & Hooper, A. Inversion of Surface Deformation Data for Rapid Estimates of Source Parameters and Uncertainties: A Bayesian Approach. *Geochem Geophys Geosyst* 19, 2194-2211 (2018).
5. Beghini, L. L., Beghini, A., Katz, N., Baker, W. F. & Paulino, G. H. Connecting architecture and engineering through structural topology optimization. *Engineering Structures* 59, 716-726 (2014).
6. Bendsøe, M. P. & Sigmund, O. Topology optimization by distribution of isotropic material. in *Topology Optimization: Theory, Methods, and Applications* (eds. Bendsøe, M. P. & Sigmund, O.) 1-69 (Springer, Berlin, Heidelberg, 2004). doi:10.1007/978-3-662-05086-6\_1.
7. Cea, J. Conception optimale ou identification de formes, calcul rapide de la dérivée directionnelle de la fonction coût. *ESAIM: Modélisation mathématique et analyse numérique* 20, 371-402 (1986).
8. Cervelli, P., Murray, M. H., Segall, P., Aoki, Y. & Kato, T. Estimating source parameters from deformation data, with an application to the March 1997 earthquake swarm off the Izu Peninsula, Japan. *Journal of Geophysical Research: Solid Earth* 106, 11217-11237 (2001).
9. Charco, M. & Galán del Sastre, P. Efficient inversion of three-dimensional finite element models of volcano deformation. *Geophysical Journal International* 196, 1441-1454 (2014).
10. Dapogny, C. & Bonnetier, E. An introduction to shape and topology optimization. <https://membres-ljk.imag.fr/Charles.Dapogny/coursoptim.html>.
11. Dapogny, C. & Feppon, F. Shape optimization using a level set based mesh evolution method: an overview and tutorial. *Comptes Rendus. Mathématique* 361, 1267-1332 (2023).
12. Dapogny, C. & Feppon, F. dapogny/sotuto. (2024).
13. Dapogny, C., Lebbe, N. & Oudet, E. Optimization of the shape of regions supporting boundary conditions. *Numer. Math.* 146, 51-104 (2020).
14. Dzurisin, D. *Volcano Deformation: Geodetic Monitoring Techniques*. (Springer ; Praxis, Berlin ; New York : Chichester, UK, 2007).
15. Feppon, F., Allaire, G., Bordeu, F., Cortial, J. & Dapogny, C. Shape optimization of a coupled thermal fluid-structure problem in a level set mesh evolution framework. *SeMA* 76, 413-458 (2019).
16. Feppon, F., Allaire, G., Dapogny, C. & Jolivet, P. Topology optimization of thermal fluid-structure systems using body-fitted meshes and parallel computing. *Journal of Computational Physics* 417, 109574 (2020).
17. Frei, W. Designing New Structures with Shape Optimization. COMSOL <https://www.comsol.com/blogs/designing-new-structures-with-shape-optimization> (2015).
18. Geuzaine, C., Remacle, J.-F. & Dular, P. Gmsh: a three-dimensional finite element mesh generator. *International Journal for Numerical Methods in Engineering* 79, 1309-1331 (2009).
19. Greiner, S. H. Including topography and a 3D-elastic structure into a Finite-Element deformation model of Grímsvötn, Iceland. (2021).
20. Hadamard, J. *Mémoire Sur Le Problème d'analyse Relatif a l'équilibre Des Plaques Élastiques Encastrees*. (Imprimerie nationale, 1908).
21. Hecht, F. New development in FreeFem++. *J. Numer. Math.* 20, 251-265 (2012).
22. Hickey, J. & Gottsmann, J. Benchmarking and developing numerical Finite Element models of volcanic deformation. *Journal of Volcanology and Geothermal Research* 280, 126-130 (2014).
23. Hunter, W. & others. ToPy - topology optimization with python. (2017).
24. Jensen, J. s. & Sigmund, O. Topology optimization for nano-photonics. *Laser & Photonics Reviews* 5, 308-321 (2011).
25. Le Quilliec, G. Topology optimization procedure TOPOPTIM and other various developments made with Cast3M. (2014) doi:10.13140/2.1.2718.3682.
26. McTigue, D. F. Elastic stress and deformation near a finite spherical magma body: Resolution of the point source paradox. *J. Geophys. Res.* 92, 12931-12940 (1987).
27. Mogi, K. Relations between the eruptions of various volcanoes and the deformations of the ground surfaces around them. *Earthq Res Inst* 36, 99-134 (1958).

# References - II

28. Parks, M. et al. Data and geodetic modelling results for Science article 'Fracturing and tectonic stress drives ultra-rapid magma flow into dikes'. (2024).
29. Segall, P. Earthquake and Volcano Deformation. (Princeton university press, Princeton, N. J, 2010).
30. Sigmund, O. A 99 line topology optimization code written in Matlab. *Struct Multidisc Optim* 21, 120–127 (2001).
31. Sigmund, O. & Maute, K. Topology optimization approaches: A comparative review. *Struct Multidisc Optim* 48, 1031–1055 (2013).
32. Sigmundsson, F. et al. Intrusion triggering of the 2010 Eyjafjallajökull explosive eruption. *Nature* 468, 426–430 (2010).
33. Sigmundsson, F. et al. Fracturing and tectonic stress drives ultrarapid magma flow into dikes. *Science* eadn2838 (2024) doi:10.1126/science.adn2838.
34. Sigmundsson, F. et al. Chapter 11 - Magma Movements in Volcanic Plumbing Systems and their Associated Ground Deformation and Seismic Patterns. in *Volcanic and Igneous Plumbing Systems* (ed. Burchardt, S.) 285–322 (Elsevier, 2018). doi:10.1016/B978-0-12-809749-6.00011-X.
35. Slavov, S. & Konsulova-Bakalova, M. Optimizing Weight of Housing Elements of Two-stage Reducer by Using the Topology Management Optimization Capabilities Integrated in SOLIDWORKS: A Case Study. *Machines* 7, 9 (2019).
36. Taylor, N. C., Johnson, J. H. & Herd, R. A. Making the most of the Mogi model: Size matters. *Journal of Volcanology and Geothermal Research* 419, 107380 (2021).
37. Trasatti, E. Volcanic and Seismic Source Modeling: An Open Tool for Geodetic Data Modeling. *Front. Earth Sci.* 10, (2022).
38. Valssson, G. P. ISN2016 - Tækniðskýrsla. <https://www.lmi.is/is/um-lmi/frettagfirlit/isn2016-tkniskrsla> (2019).
39. Velez, M. L., Euillades, P., Caselli, A., Blanco, M. & Díaz, J. M. Deformation of Copahue volcano: Inversion of InSAR data using a genetic algorithm. *Journal of Volcanology and Geothermal Research* 202, 117–126 (2011).
40. Yang, X.-M., Davis, P. M. & Dieterich, J. H. Deformation from inflation of a dipping finite prolate spheroid in an elastic half-space as a model for volcanic stressing. *Journal of Geophysical Research: Solid Earth* 93, 4249–4257 (1988)
28. Parks, M. et al. Data and geodetic modelling results for Science article 'Fracturing and tectonic stress drives ultra-rapid magma flow into dikes'. (2024).
29. Segall, P. Earthquake and Volcano Deformation. (Princeton university press, Princeton, N. J, 2010).
30. Sigmund, O. A 99 line topology optimization code written in Matlab. *Struct Multidisc Optim* 21, 120–127 (2001).
31. Sigmund, O. & Maute, K. Topology optimization approaches: A comparative review. *Struct Multidisc Optim* 48, 1031–1055 (2013).
32. Sigmundsson, F. et al. Intrusion triggering of the 2010 Eyjafjallajökull explosive eruption. *Nature* 468, 426–430 (2010).
33. Sigmundsson, F. et al. Fracturing and tectonic stress drives ultrarapid magma flow into dikes. *Science* eadn2838 (2024) doi:10.1126/science.adn2838.
34. Sigmundsson, F. et al. Chapter 11 - Magma Movements in Volcanic Plumbing Systems and their Associated Ground Deformation and Seismic Patterns. in *Volcanic and Igneous Plumbing Systems* (ed. Burchardt, S.) 285–322 (Elsevier, 2018). doi:10.1016/B978-0-12-809749-6.00011-X.
35. Slavov, S. & Konsulova-Bakalova, M. Optimizing Weight of Housing Elements of Two-stage Reducer by Using the Topology Management Optimization Capabilities Integrated in SOLIDWORKS: A Case Study. *Machines* 7, 9 (2019).
36. Taylor, N. C., Johnson, J. H. & Herd, R. A. Making the most of the Mogi model: Size matters. *Journal of Volcanology and Geothermal Research* 419, 107380 (2021).
37. Trasatti, E. Volcanic and Seismic Source Modeling: An Open Tool for Geodetic Data Modeling. *Front. Earth Sci.* 10, (2022).
38. Valssson, G. P. ISN2016 - Tækniðskýrsla. <https://www.lmi.is/is/um-lmi/frettagfirlit/isn2016-tkniskrsla> (2019).
39. Velez, M. L., Euillades, P., Caselli, A., Blanco, M. & Díaz, J. M. Deformation of Copahue volcano: Inversion of InSAR data using a genetic algorithm. *Journal of Volcanology and Geothermal Research* 202, 117–126 (2011).
40. Yang, X.-M., Davis, P. M. & Dieterich, J. H. Deformation from inflation of a dipping finite prolate spheroid in an elastic half-space as a model for volcanic stressing. *Journal of Geophysical Research: Solid Earth* 93, 4249–4257 (1988).

A wide-angle photograph of a natural landscape. In the foreground, there is a field of tall, dry grass. Beyond the grass, a body of water, possibly a lake or a wide river, stretches across the middle ground. In the background, there are several mountain ranges. The mountains on the left appear to have some snow or ice on their peaks. The sky is filled with various types of clouds, from wispy cirrus to thicker cumulus, with some sunlight breaking through to illuminate parts of the clouds and the tops of the mountains.

Thank you!